LA UR-91-3522

The Kaon B-parameter with Wilson Fermions

Rajan Gupta and David Daniel

T-8, MS-B285, Los Alamos National Laboratory, Los Alamos, NM 87545

Gregory W. Kilcup

Physics Department, The Ohio State University, Columbus, OH 43210

Apoorva Patel

Supercomputer Education and Research Centre and Centre for Theoretical Studies
Indian Institute of Science, Bangalore 560012, India

Stephen R. Sharpe

Physics Department FM-15, University of Washington, Seattle, WA 98195

We calculate the kaon B-parameter in quenched lattice QCD at $\beta = 6.0$ using Wilson fermions at $\kappa = 0.154$ and 0.155. We use two kinds of non-local ("smeared") sources for quark propagators to calculate the matrix elements between states of definite momentum. The use of smeared sources yields results with much smaller errors than obtained in previous calculations with Wilson fermions. By combining results for $\vec{p} = (0,0,0)$ and $\vec{p} = (0,0,1)$, we show that one can carry out the non-perturbative subtraction necessary to remove the dominant lattice artifacts induced by the chiral symmetry breaking term in the Wilson action. Our final results are in good agreement with those obtained using staggered fermions. We also present results for B-parameters of the $\Delta I = 3/2$ part of the electromagnetic penguin operators, and preliminary results for B_K in the presence of two flavors of dynamical quarks.

11 October 1992

1. Introduction

Present calculations of weak matrix elements in the quenched approximation with Wilson fermions suffer from two main sources of error: (i) the signal is poor and (ii) there are large $O(a)$ corrections due to lack of chiral symmetry [1] [2]. In this paper we investigate the calculation of the matrix elements of four-fermion operators between pseudoscalar states, and in particular B_K. To improve the signal we calculate the 3-point function by sandwiching the operator between kaons produced by smeared sources. This trick has been used to obtain very accurate results with staggered fermions [3]. In order to reduce the $O(a)$ artifacts we use a momentum-subtraction technique similar to that tried earlier by the ELC collaboration [4]. We find that the combined method reduces the statistical errors for all four-fermion operators we have looked at, and allows us to perform non-perturbative subtractions for removing two of the three chiral symmetry violating terms in B_K.

The $O(a)$ corrections arise due to mixing between operators of different tensor structure induced by the explicit chiral symmetry breaking term introduced by Wilson to remove lattice doublers. In principle this mixing can be calculated in perturbation theory, but there are large non-perturbative effects at values of g used in lattice calculations. There are two approaches to improving the situation: one is to work with an improved action so that the mixing occurs at $O(g^2a)$ and $O(a^2)$ rather than at $O(a)$ [5], and the second is to devise non-perturbative methods to subtract off the lattice artifacts. It is likely that the eventual solution will be a combination of the two methods. To this end we demonstrate that the calculation of matrix elements within states of definite lattice momentum works for $\vec{p} = (0,0,0)$ and $(0,0,1)$, and furthermore that one can reliably carry out a non-perturbative subtraction using these two values of momentum. We use the kaon B-parameter as the testing ground for two reasons: (a) there are very accurate results available using staggered fermions on the same set of lattices against which we may compare our results, and (b) there is no mixing with operators of lower dimension.

To make our non-perturbative method work we need two kinds of hadron source: one that produces hadrons with zero momentum and the other that couples to all momenta. We construct zero momentum hadron correlators using wall source quark propagators, while the Wuppertal source [6] propagators yield hadron correlators that have overlap with all momenta. We have shown in Ref. [7] that these two kinds of correlators yield reliable signals for both the amplitude and the mass extracted from 2-point correlation

functions. That paper describes in detail the lattices used in the calculation and details of the quark propagators and hadron correlators. It also contains results for hadron masses and decay constants obtained from 2-point correlation functions. We use 35 lattices of size $16^3 \times 40$ at $\beta \equiv 6g^{-2} = 6.0$ with quark propagators calculated at $\kappa = 0.154$ and 0.155. The two values of κ correspond to kaons of mass $M_K = 700$ MeV and 560 MeV respectively, using $a^{-1} = 1.9$ GeV.

The most accurate results for B_K at $\beta = 6.0$ have been obtained with staggered fermions [3]:

$$B_K = \begin{cases} 0.70 \pm 0.02 \ : \ (16^3 \times 40 \text{ lattices}) \\ 0.70 \pm 0.01 \ : \ (24^3 \times 40 \text{ lattices}) \end{cases} . \tag{1.1}$$

There are two previous estimates of B_K with Wilson fermions at $\beta = 6.0$. The results of Bernard and Soni are [2]:

$$B_K = \begin{cases} 0.83 \pm 0.11 \pm 0.11 \ : \ (16^3 \times 40 \text{ lattices}) \\ 0.66 \pm 0.08 \pm 0.04 \ : \ (24^3 \times 40 \text{ lattices}) \end{cases} , \tag{1.2}$$

and that of the ELC collaboration is [1]:

$$B_K = 0.81 \pm 0.16 \pm 0.06 \ : \ (10^2 \times 20 \times 40 \text{ lattices}) , \tag{1.3}$$

where the second error is an estimate of the systematic error due to the subtraction of the bad chiral behavior. In all calculations the lattice kaon consisted of two almost degenerate quarks (the ratio $m_s/m_u \leq 3$). The above results were obtained after interpolation/extrapolation of the lattice data to a kaon mass of 495 MeV. The large spread in these numbers and the systematic errors due to bad chiral behavior induced by the Wilson term underscore the need for further improvements and new methods.

We also calculate the B-parameter for the $\Delta I = 3/2$ part of the electromagnetic penguin operators $\mathcal{O}_7$ and $\mathcal{O}_8$. Previous calculations with both Wilson [8] [9], and staggered fermions [10] show that reliable results for the matrix elements of these LR operators can be obtained in lattice calculations and that the vacuum saturation approximation (VSA) provides a good estimate, *i.e.* $B_{7,8}^{3/2} = 1.0 \pm 0.1$. Our estimates are 0.89(4) and 0.93(5) respectively, and we find that the dominant contribution to the matrix elements of both the LR operators and their VSA comes from the pseudoscalar $\otimes$ pseudoscalar ($\mathcal{P}$) part of the 4-fermion operator. Our data show that matrix elements of $\mathcal{P}$ are larger by a factor of 10 or more than other tensor structures and that the 2-color loop contraction is roughly three times larger than the 1-color loop. Furthermore, as the operator $\mathcal{P}$ is not suppressed

in the chiral limit, we believe that VSA will be a good approximation in cases where the operator or its fierz transform contains $\mathcal{P}$ at tree level.

This paper is organized as follows: in Section 2 we review the problem induced by the Wilson r term and our partial solution for subtracting lattice artifacts. In Section 3 we describe the lattice methods and in Section 4 we present our results for B_K. We make a comparison with earlier results obtained with both Wilson and staggered fermions in Section 5. Section 6 presents preliminary results for B_K with two flavors of dynamical quarks. The analysis of the LR operators is given in Section 7 and we end with conclusions in Section 8.

2. B_K and the problem of bad chiral behavior

Weak interactions give rise to mixing between the K^0 and $\overline{K^0}$. The relevant operator in the low energy effective weak Hamiltonian is the $\Delta S = 2$ four-fermion operator $(\bar{s}\gamma_\mu Ld)(\bar{s}\gamma_\mu Ld)$, where we use the notation $L = (1-\gamma_5)$ and $R = (1+\gamma_5)$. The value of the matrix element of this operator between a K^0 and $\overline{K^0}$ at a typical hadronic scale is severely influenced by strong interaction effects. It has become customary to parameterize this matrix element by the kaon B-parameter, B_K, which measures the deviation from its value in the VSA:

$$\left\langle \overline{K^0}\right|(\bar{s}\gamma_\mu Ld)(\bar{s}\gamma_\mu Ld)\left|K^0\right\rangle = \frac{8}{3} f_K^2 M_K^2 B_K, \tag{2.1}$$

where () indicates a trace over the spin and color indices. The normalization used for the decay constant is such that $f_\pi = 132$ MeV. If the VSA is exact then $B_K = 1$. To calculate B_K from first principles we must turn to non-perturbative methods such as the lattice. Our lattice calculation of B_K uses Wilson's formulation for fermions. The inherent violation of chiral symmetry in this approach leads to technical difficulties which we now review.

To begin with, note that $(\bar{s}\gamma_\mu Ld)(\bar{s}\gamma_\mu Ld)$ is a special case of the operator

$$\mathcal{O}_+ = \frac{1}{2}\big((\bar{\psi}_1\gamma_\mu L\psi_2)(\bar{\psi}_3\gamma_\mu L\psi_4) + (2 \leftrightarrow 4)\big), \tag{2.2}$$

with $\psi_1 = \psi_3 = s$ and $\psi_2 = \psi_4 = d$. The significance of this is that with a chirally invariant regulator $\mathcal{O}_+$ is multiplicatively renormalized. With Wilson fermions, however, this is not the case: there is mixing of this LL operator with other tensor structures in addition to an overall renormalization, and this complicates the definition of a lattice operator with

the desired continuum behavior. In perturbation theory, the corrected operator has been calculated to 1-loop in Refs. [11] and [12]:

$$\mathcal{O}_+^{\rm cont} = \big(1 + \frac{g^2}{16\pi^2} Z_+(r, a\mu)\big)\mathcal{O}_+^{\rm latt} + \frac{4g^2}{16\pi^2}\, r^2 Z^*(r)\big(\mathcal{O}_+^{STP} + \mathcal{O}_+^{VA} + \mathcal{O}_+^{SP}\big) \tag{2.3}$$

where

$$\begin{aligned}
\mathcal{O}_+^{STP} &= \frac{N-1}{16N}\big[(\mathcal{S}+\mathcal{T}+\mathcal{P}) + (2 \leftrightarrow 4)\big], \\
\mathcal{O}_+^{VA} &= -\frac{N^2+N-1}{32N}\big[(\mathcal{V}-\mathcal{A}) + (2 \leftrightarrow 4)\big], \\
\mathcal{O}_+^{SP} &= -\frac{1}{16N}\big[(\mathcal{S}-\mathcal{P}) + (2 \leftrightarrow 4)\big],
\end{aligned} \tag{2.4}$$

and $N = 3$ is the number of colors. We have used a condensed notation for the allowed Lorentz tensor structures:

$$\begin{aligned}
\mathcal{S} &= (\bar\psi_1\psi_2)(\bar\psi_3\psi_4), \\
\mathcal{V} &= (\bar\psi_1\gamma_\mu\psi_2)(\bar\psi_3\gamma_\mu\psi_4). \\
\mathcal{T} &= \sum_{\mu<\nu}(\bar\psi_1\sigma_{\mu\nu}\psi_2)(\bar\psi_3\sigma_{\mu\nu}\psi_4), \\
\mathcal{A} &= (\bar\psi_1\gamma_\mu\gamma_5\psi_2)(\bar\psi_3\gamma_\mu\gamma_5\psi_4), \\
\mathcal{P} &= (\bar\psi_1\gamma_5\psi_2)(\bar\psi_3\gamma_5\psi_4),
\end{aligned} \tag{2.5}$$

where γ_μ, γ_5 are hermitian and $\sigma_{\mu\nu} = (\gamma_\mu\gamma_\nu - \gamma_\nu\gamma_\mu)/2$. We note that the Fierz transform eigenstates appearing in Eq. (2.3) are only $(\mathcal{V}+\mathcal{A})$, $\frac{1}{2}(\mathcal{V}-\mathcal{A})\pm(\mathcal{S}-\mathcal{P})$ and $(\mathcal{S}+\mathcal{T}+\mathcal{P})$; there is also no mixing between the fifth eigenstate of the Fierz transformation $(\mathcal{S}-\frac{1}{3}\mathcal{T}+\mathcal{P})$ and the operator $\mathcal{O}_+$ at 1-loop. There is no mixing with lower dimensional operators, for the simple reason that there are *no* $\Delta S = 2$ operators of lower dimension. We shall henceforth denote the perturbatively corrected $(\bar s\gamma_\mu L d)(\bar s\gamma_\mu L d)$ operator (cf. Eq. (2.3)) by $\hat{\mathcal{O}}$.

The renormalization coefficients for Wilson parameter $r = 1$ are given in Table 1 in three schemes: the dimensional reduction ($DRED$) used by Altarelli *et al.* [13] and Martinelli [11], as well as the "naive" dimensional regularization (NDR) and the dimensional reduction ($DR(\overline{EZ})$) scheme used by Bernard *et al.* in [12]. A detailed description of $DRED$ and NDR schemes and their relative advantages and disadvantages is given in Ref. [14]. We tabulate the relevant results in order to provide easy reference, and to allow the reader to make a rough estimate of the magnitude of the scheme dependence. All our results are given in the $DRED$ scheme, except when we compare raw lattice numbers against those in Ref. [15], in which case we use $DR(\overline{EZ})$.

For each of the four-fermion operators, $\mathcal{S}$, $\mathcal{V}$, $\mathcal{T}$, $\mathcal{A}$, and $\mathcal{P}$, there are two distinct contractions with the external states. In the first each bilinear is contracted with an incoming or outgoing kaon corresponding to two spin and two color traces. We label these contractions by $\mathcal{P}^2$, $\mathcal{S}^2$, $\mathcal{V}^2$, $\mathcal{A}^2$ and $\mathcal{T}^2$. The other contraction consists of a single spin and color trace which we Fierz transform to two spinor loops. We label them by $\mathcal{P}^1$, $\mathcal{S}^1$, $\mathcal{V}^1$, $\mathcal{A}^1$ and $\mathcal{T}^1$, since they have a single color trace. We will find it useful to further split the $\mathcal{V}$, $\mathcal{A}$ and $\mathcal{T}$ terms into their space and time components, and denote these components by subscripts s and t respectively. This notation is similar to that used with staggered fermions [3] and will facilitate later comparison of results for individual operators between the two formulations.

In order to extract B_K, we calculate, at non-zero momentum transfer, the matrix element

$$\mathcal{M}_K(\vec{p}) = \left\langle \overline{K^0}(\vec{p}) \middle| \hat{\mathcal{O}}(\vec{p}) \middle| K^0(\vec{p}=0) \right\rangle. \tag{2.6}$$

In chiral perturbation theory $\mathcal{M}_K(\vec{p})$ behaves as $\sim \gamma_K p_K \cdot p_{\bar{K}}$, where $\gamma_K = 8/3\, f_K^2 B_K$, and p_K and $p_{\bar{K}}$ are the on-shell four-momenta of the external states, so that $p_K \cdot p_{\bar{K}} = M_K\sqrt{M_K^2 + (\vec{p})^2}$. Unfortunately, on the lattice with Wilson fermions chiral symmetry is explicitly broken and the expansion becomes

$$\mathcal{M}_K(\vec{p}) = \alpha + \beta M_K^2 + (\gamma + \gamma_K) p_K \cdot p_{\overline{K}} + \ldots. \tag{2.7}$$

Here the terms proportional to α, β and γ are unphysical contributions arising due to the r-term in the Wilson action, and suppressed by one power of the lattice spacing a. Similar formulae hold for each individual spin-color term described above, and apply to both the on-shell ($\langle \overline{K^0}|\hat{\mathcal{O}}|K^0\rangle$) and the off-shell ($\langle 0|\hat{\mathcal{O}}|K^0 K^0\rangle$) matrix elements.

Using $\hat{\mathcal{O}}$ should reduce the lattice artifacts, but it will not eliminate them completely because it is only an approximation to the operator with the desired continuum behavior. In particular, the coefficients Z contain terms of $\mathcal{O}(g^4)$ and higher that have not been calculated, and, more importantly, as previous calculations have shown, there are large non-perturbative effects. We therefore require non-perturbative methods to isolate the physical coefficient γ_K.

The most troublesome of the lattice artifacts is α. Failure to correctly subtract this contamination will mean that B_K will diverge in the chiral limit. To eliminate this, it is not

necessary to work at non-zero momentum transfer. One can simply calculate $\mathcal{M}_K(\vec{p}=0)$ at different values of κ (that is, different values of M_K) and take a difference, leaving

$$\mathcal{M}_K(\kappa,\vec{p}=0)-\mathcal{M}_K(\tilde{\kappa},\vec{p}=0)=(\beta+\gamma+\gamma_K)(M_K^2-\tilde{M}_K^2). \tag{2.8}$$

To remove β one takes the difference of the on-shell and off-shell matrix elements. This method has been used in Refs. [1] and [2], and suffers from the lack of control over final state interactions between the kaons in the off-shell amplitude. A review of the status of previous results is given in Refs. [16] and [17].

We advocate using momentum subtraction which eliminates both α *and* β at a fixed value of M_K, using only on-shell quantities. For example, by calculating the matrix element of $\hat{\mathcal{O}}$ for two different values of $\vec{p}$ and taking the difference one gets

$$\mathcal{M}_K(\vec{p})-\mathcal{M}_K(0)=(\gamma+\gamma_K)M_K(E(p)-M_K)+\ldots. \tag{2.9}$$

In practice we calculate

$$B_K=\frac{E(p)\,B_K^L(p)-M_K\,B_K^L(0)}{E(p)-M_K}=(\gamma+\gamma_K)+\ldots \tag{2.10}$$

at each value of κ, where by $B_K^L(p)$ we mean the ratio of the matrix element to its VSA value, both calculated on the lattice at appropriate momentum transfer.

This momentum subtraction scheme does not eliminate the lattice artifact γ. Furthermore, in working at non-zero momentum there is a danger that higher order terms (for example quartic in momenta) omitted in Eq. (2.7) may become significant. Therefore in order to compare the lattice result with experiment we have to make the following assumptions: (i) using the perturbatively improved operator $\hat{\mathcal{O}}$ makes γ negligible; (ii) the terms of order p^4 and higher that we have neglected in the chiral expansion do not have large coefficients. The first assumption is expected to become more reliable on using an improved Wilson action, while the second will come under better control as calculations are done on larger spatial lattices since then the gap between lattice momenta will decrease. At this stage the only justification for these assumptions is the a posteriori agreement of results with those obtained using staggered fermions.

3. Methodology

Our method for calculating B_K requires that we double the $16^3 \times 40$ lattices in the time direction, so that they are of size $16^3 \times 80$. On these doubled lattices we construct hadron correlators such that the correlator on time slices 1–39 is the forward moving particle with the source at time slice 0, while the correlator on time slices 79–41 is the backward moving particle with the periodically reflected source on time slice 80. To calculate matrix elements we insert the operator between these "forward" and "backward" moving particles on the original $16^3 \times 40$ lattices.

In practice, we divide the correlators for the various matrix elements by the product of kaon correlators, so that we directly obtain the B-parameters for the various operators $\mathcal{O}$

$$B_{\mathcal{O}} \equiv \frac{3}{8} \frac{\langle \overline{K^0}(\vec{p}) | \mathcal{O} | K^0(\vec{p}=0) \rangle}{\langle \overline{K^0}(\vec{p}) | A_4 | 0 \rangle \langle 0 | A_4 | K^0(\vec{p}=0) \rangle}. \tag{3.1}$$

We can select the kaon momenta by our choice of source and by inserting momentum into the operator $\mathcal{O}$. The statistical errors are reduced because we can average the operator location over a time slice of the lattice. Away from the sources, only the lightest state contributes to the correlators, and we should find a time-independent plateau giving $B_{\mathcal{O}}$. This method is similar to the one we have used successfully with staggered fermions [3].

The physical picture of the process for calculating matrix elements using smeared sources is as follows: a wall source at $t = 0$ produces zero momentum K^0 which propagates for a time t, at which point the operator inserts momentum $\vec{p}$, and the resulting $\overline{K^0}$ with momentum $\vec{p}$ then propagates the remaining (N_t-t) time slices until it is destroyed by a Wuppertal source. Three factors are essential for our method to work:

(i) The wall source creates only zero-momentum kaons; otherwise there is contamination from matrix elements of kaons with other momenta.

(ii) The Wuppertal source has significant overlap with the lowest few momenta allowed on the lattice.

(iii) For matrix elements involving $\vec{p} \neq 0$ kaons, we must ensure that there exists an overlap region for the kaons where a plateau can be observed in the B-parameter signal. Thus it is essential that the signal for the zero-momentum kaon produced by the wall source extends across the lattice to the region where there is a signal for the non-zero momentum kaon produced by the Wuppertal source.

In Ref. [7] we showed that these conditions are satisfied by the Wuppertal and wall correlators, when we use $\vec{p} = (0,0,0)$ and $\vec{p} = (0,0,1)$. Furthermore, there are a number of consistency checks we make:

(1) The $\vec{p} = 0$ matrix element is calculated three different ways; (a) using wall sources on both sides, (b) using wall source on one side and Wuppertal source on the other, and (c) using Wuppertal sources on both sides (in this case there is a small contamination from the $\vec{p} = (0,0,1)$ state).

(2) We use two kaon source operators: γ_5 and A_4. The plateau in each individual $B_{\mathcal{O}}$ is reached from opposite directions for these two. The two results should converge to the same value.

As shown in Tables 2a–3b, these checks are satisfied by our data within the statistical accuracy. We also find that the B-parameter for the operators $\mathcal{A}_t^2$ and $\mathcal{P}^2$ are within a factor of two of their VSA values. As in the case of staggered fermions, the final value of B_K is obtained after a large cancellation between the $\mathcal{A}$ and $\mathcal{V}$ components showing that VSA is not a good approximation.

4. Results for B_K

Our final lattice result at a given value of κ and $\vec{p}$ is obtained from the perturbatively improved combination (using the convention that all four quarks have distinct flavor labels so that each term has just one Wick contraction)

$$\begin{aligned} Z_A^2 B_K^L(\vec{p}) =& \left(1 + \frac{g^2}{16\pi^2} Z_+(r, a\mu)\right)\Big[\mathcal{V}^1 + \mathcal{V}^2 + \mathcal{A}^1 + \mathcal{A}^2\Big] \\ &+ \frac{g^2}{16\pi^2}\,\frac{r^2 Z^*(r)}{12}\Big[(26\mathcal{S}^1 + 2\mathcal{S}^2) - (18\mathcal{P}^1 - 6\mathcal{P}^2) \\ &\qquad + 4(\mathcal{T}^1 + \mathcal{T}^2) + (\mathcal{V}^1 - \mathcal{A}^1) - 11(\mathcal{V}^2 - \mathcal{A}^2)\Big]. \end{aligned} \tag{4.1}$$

For simplicity, we have here used the operator symbol to denote its B-parameter. The 1-loop perturbative results for the renormalization constants Z_A and Z_+ are given in Table 1. Note that the finite part of the renormalization factor $(1 + \frac{g^2}{16\pi^2} Z_+)$ is largely canceled by Z_A^2 for $g^2 \lesssim 1$.

We give the results for the individual $B_{\mathcal{O}}$ (without any g^2 corrections) at $\kappa = 0.154$ and 0.155 in Tables 2a–3b. In all cases we find that the signal in the ratio of correlators is significantly better with the operator γ_5 as the kaon source than with the operator A_4,

even though the two sets give consistent results. As an example, we show a comparison of the two signals in Figs. 1a and 1b. Our final results therefore use the γ_5 numbers. We point out that in case of non-zero momentum transfer, the signal for $B_{\mathcal{O}}$ only exists closer to the Wuppertal source (at time slice "40") than the wall source (at time-slice "0"). This is because the signal in the $\vec{p} = (0, 0, 1)$ kaon correlators only extends for about 20 time-slices. The overall quality of the signal for B_K^L (with $g^2 = 1, \mu a = 1.0$) is shown in Figs. 1, 2, 3 and 4 at various values of κ and $\vec{p}$.

Tables 2a–3b show that all individual $B_{\mathcal{O}}$, except for $B_{\mathcal{A}_t}$, increase by a factor of about 2 between $\kappa = 0.154$ and 0.155. This increase is largely due to the change in VSA, *i.e.* the factor $f_K^2 M_K^2$ decreases by approximately 1.9 between the two κ values [7]. This shows that at these values of κ, the lattice matrix elements are dominated by the constant term α.

The contribution of the mixing terms to B_K^L can be large only if the matrix elements are large, since the perturbative mixing coefficient is ≈ 0.005 for $g^2 = 1$. The data show that the largest matrix elements are of the operator $\mathcal{P}$; however their net contribution to B_K^L is very small, since $\mathcal{P}^2 \sim 3\mathcal{P}^1$ (approximate VSA). Both $\mathcal{T}^2$ and $\mathcal{V}^2$ are close to zero. The next largest contribution comes from $4\mathcal{T}^1$, which is partially canceled by $26\mathcal{S}^1 + 2\mathcal{S}^2$. The net result of these features in the data is that the contribution of mixing terms to B_K is in fact of the order of a few percent. Unfortunately, since the unphysical term γ in Eq. (2.7) also gets contributions from the diagonal operators, the small value of the mixing terms does not provide a bound on γ.

Given $B_K^L(\vec{p})$ we calculate B_K and the errors using Eq.(2.10) two ways: (1) for each jackknife sample we first perform the momentum subtraction and then the mean value and the error are obtained as the jackknife estimate over the 35 samples, and (2) we construct the four quantities needed in Eq. (2.10) independently along with their errors, and obtain the final error estimate assuming that the individual estimates are uncorrelated. Our quoted results use the first method, but we note that both the methods yield consistent estimates.

We have calculated $B_K^L(\vec{p} = (0, 0, 0))$ three different ways: using Wuppertal-Wuppertal $(S - S)$, Wuppertal-wall $(S - W)$, and wall-wall $(W - W)$ correlators. For example, our

results, using $g^2 = 1.0$ and $\mu a = 1.0$, are:

$$B_K^L(\kappa = 0.154) = \begin{cases} 0.38(7) \ : \ S-S \\ 0.37(4) \ : \ S-W \\ 0.37(4) \ : \ W-W \end{cases} ,$$
$$B_K^L(\kappa = 0.155) = \begin{cases} 0.10(11) \ : \ S-S \\ 0.11(7) \ : \ S-W \\ 0.13(7) \ : \ W-W \end{cases} . \tag{4.2}$$

The consistency of the data suggests that the contamination in the $S-S$ result from higher momentum kaon states is at most a few percent. Since only the $S-W$ correlators give results at both $\vec{p} = (0,0,0)$ and $(0,0,1)$, we shall henceforth quote results for $B_K^L(\vec{p})$ obtained from these.

In order to extract the continuum result for B_K we must choose the values of both g^2 and μa to use in Eq. (4.1). Lepage and Mackenzie have suggested [18] that perturbation theory is much better behaved if one uses the coupling constant in a continuum scheme such as $\overline{MS}$, instead of the bare lattice g^2. They also give a prescription for choosing the appropriate scale of the coupling constant. In general this scale will differ for the various operators that mix with $\mathcal{O}_+$ in Eq. (4.1). To simplify the calculation we take all the scales, and thus all the coupling constants, to be the same, *i.e.* all of $O(\pi/a)$. Then the Lepage-Mackenzie prescription amounts to a replacement of the bare lattice g^2 with an effective coupling $g^2_{\rm eff} \approx 1.75 g^2$ at $\beta = 6.0$. To study the dependence on $g^2_{\rm eff}$, we use four different values, $g^2_{\rm eff} = 0.0$, 1.0, 1.338 and 1.75. It is important to realize that only a 2-loop calculation of the perturbative coefficients can test whether a given choice for $g^2_{\rm eff}$ is reasonable. Such calculations that have been done to date support Lepage-Mackenzie prescription for choosing $g^2_{\rm eff}$ [18].

The choice of μa is of a different character to that of g^2. In physical matrix elements (e.g. that related to CP-violation in $K^0 - \bar{K^0}$ mixing) B_K always appears multiplied by a coefficient function, such that the combination is independent of μ. At leading order, the scale independent combination is

$$\widehat{B}_K = \alpha_s(\mu)^{-6/(33-2N_f)} B_K(\mu) \ , \tag{4.3}$$

where N_f is the number of active flavors. In fact, $\widehat{B}_K$ does have some dependence on μ, coming from the following sources. First, since we are using only the leading order expression for $Z(\mu a)$, $\widehat{B}_K$ does depend on μ at non-leading order: $d \ln \widehat{B}_K / d \ln \mu \propto g^4(\mu)$. This is likely to be a small effect, and it can probably be pushed to next order given the fact

that the two-loop anomalous dimension and one-loop matching coefficients are known. We say "probably" because it is possible that there are some residual subtleties with Wilson fermions associated with the mixing of $\mathcal{O}_+$ with opposite chirality operators. A related source of μ dependence occurs when μa differs greatly from unity: then higher order terms, proportional to $[g^2 \ln(\mu a)]^n$, which are not included in Eq. (4.1), become large. What is happening is that the leading logarithms, which have been summed into the coefficient function, are partially incorporated into the perturbative coefficients. Once again, one can probably take these into account knowing the anomalous dimension to 2-loops, or finesse the problem by taking $\mu a \sim 1$. Finally, we are calculating the lattice result in the quenched approximation, for which the number of active flavors is zero, while we wish to match to the full theory with N_f active flavors. This introduces a small μ dependence.

Our emphasis in this paper is on improving methods for calculating B_K, and not on extracting final numbers for $\widehat{B}_K$. Thus we choose to quote our results for a variety of values of μa so as to allow others some flexibility if they wish to use our numbers. We use $\mu a = 1.0,\ \pi$, and 1.7π. We have a slight preference for $\mu a = \pi$, since then the continuum and lattice cut-offs are matched.

Table 4 shows the sensitivity of the results to the choices of parameters, for both B_K^L and the momentum subtracted B_K. There is a significant variation of the results with $g^2_{\rm eff}$ and μa. For a fixed value of μa, the lattice results for both $B_K^L(\vec{p} = (0,0,0))$ and $B_K^L(\vec{p} = (0,0,1))$ increase as a function of $g^2_{\rm eff}$ due to the increased contribution of the mixing operators. For fixed $g^2_{\rm eff}$, an increase in μa decreases the contribution of the diagonal operators (note that $B_K^L(\vec{p} = (0,0,0))$ at $\kappa = 0.155$ is insensitive to changes in μa because the diagonal contribution happens to be almost zero there).

As for B_K after momentum subtraction, the estimate decreases by $10 - 20\%$, at both values of quark mass, between $g^2_{\rm eff} = 1.0$ and $g^2_{\rm eff} = 1.75$, for fixed μa. It turns out that almost all the variation comes from the diagonal renormalization constants (for example, the ratio of $(1 + (g^2/16\pi^2)Z_+)$ to Z_A^2 changes from 0.93 to 0.8), and not from operator mixing. As our present best estimates for B_K we quote the results at $g^2_{\rm eff} = 1.75$, and use $\mu a = \pi$:

$$\begin{aligned} B_K(\kappa = 0.154) &= 0.68(22)\ , \\ B_K(\kappa = 0.155) &= 0.57(23)\ . \end{aligned} \tag{4.4}$$

5. Comparison with previous calculations

The staggered fermion results for B_K [3] are statistically the most accurate and have the correct chiral behavior. At $\beta = 6.0$, the kaon mass roughly matches for staggered $m_q = (0.02 + 0.03)$ and $\kappa = 0.154$, and for staggered $m_q = (0.01 + 0.02)$ and $\kappa = 0.155$ [19]. Thus we can compare the corresponding data for B_K. This is a particularly good comparison because the two calculations have been done using the same set of background gauge configurations. Using $g^2 = 0$ in the 4-fermion renormalization constants, the staggered results are 0.76(1) and 0.72(2) to be compared with our numbers 0.83(21) and 0.77(19) respectively. A striking feature is that the errors with Wilson fermions are a factor of 10 or more larger. The data in Table 4 indicate that the errors in individual $B_K^L(p)$ are larger by about a factor of four, and the remaining factor comes from the momentum subtraction. The staggered results were obtained by making fits without including the full covariance matrix, and if we do the same for Wilson fermions then the errors in individual $B_K^L(p)$ are reduced by a factor of about two. Thus, at the level of the signal in the correlators, the smeared sources work almost as well for Wilson fermions as for staggered fermions. It is the process of momentum subtraction that leads to a significant increase in the error.

It could be argued that one should actually compare staggered numbers with our preferred results using $g^2_{\rm eff} = 1.75$ and $\mu a = \pi$, *i.e.* 0.68(22) and 0.57(23) respectively. The rationale for this is that a good choice of $g^2_{\rm eff}$ and μa aims to reduce the effects of artifacts α, β and γ. Recall that α and β are absent for staggered fermions while a γ like term exists due to operator normalization. With this choice the Wilson fermion estimates lie systematically below the staggered values. The perturbative corrections for staggered fermions, though small, have not been included in the published results of B_K [20]. Including them would decrease B_K by $\approx (2g^2_{\rm eff})\%$. The remaining difference could be due to the difference in the $O(a)$ corrections for the two fermion formulations, *e.g.* the artifact γ. In any case, it is not clear whether the difference is significant, given the size of the errors in the Wilson results and the large variation with $g^2_{\rm eff}$ and μa.

We can also make a direct comparison with results obtained by Bernard and Soni using Wilson fermions [2]. They have calculated $B_K^L(\vec{p} = 0)$ using the perturbatively improved operator on a subset of the same lattices (they used only 19 lattices as they skipped every other one in each of the two streams), and at the same two values of κ. Their method of extraction of B_K^L is described in Ref. [2], and is different than the method we have used. Using $g^2_{\rm eff} = 1.338$ and $\mu a = 1.7\pi$ their results are $B_K^L(\vec{p} = 0) = 0.36(22)$ and 0.24(45)

at $\kappa = 0.154$ and 0.155 respectively [15], to be compared with $B_K^L(\vec{p} = 0) = 0.38(5)$ and 0.11(7) obtained by us. Even after allowing for a factor of $\sim \sqrt{2}$ due to statistics, it is clear on the basis of this comparison that our use of smeared sources has reduced the errors considerably.

Though our results for B_K^L are more accurate compared to those obtained by other groups using Wilson fermions, our final results for B_K have larger errors (cf. Eq. (1.2), (1.3)). The gain due to the use of smeared sources is compensated by the increase in error due to momentum subtraction. The advantage of using momentum subtraction is that it unambiguously removes lattice artifacts α and β. Also, numerical errors in $B_K^L(\vec{p} = 1)$, as well as the contribution of quartic terms in the chiral expansion, should decrease when using a larger lattice due to the decrease in the value of lattice momenta.

One further qualitative comparison that we can make is for the B-parameters (without perturbative improvements but after momentum subtraction) of the individual space/time and 1-loop/2-loop components of the four-fermion vector and axial operators, with the corresponding results obtained using staggered fermions [3]. Such a comparison is possible because, as discussed above, the effects of operator mixing are small. This comparison provides information on the reliability of the momentum subtraction procedure for Wilson fermions. Furthermore, as explained in Ref. [21], the chiral behavior of $B_{\mathcal{V}}$ and $B_{\mathcal{A}}$ is known; both are expected to increase in magnitude with decreasing quark mass due to chiral logarithms and finite volume dependence, and can therefore provide a sensitive test at small quark masses. The results of our comparison are shown in Table 5. Though the errors in the results with Wilson fermions are much larger, it is reassuring to see that the central values are in good agreement. In fact the agreement is far more impressive than the errors would naively lead us to believe. We need to perform calculations at more values of κ and β to confirm this favorable behavior.

6. Results with two flavors of dynamical fermions

We have also estimated B_K, using the same methodology as above, on 16^4 lattice configurations generated with two flavors of dynamical Wilson quarks. The details of these lattices are given in Ref. [22]. The kaon mass at $\beta = 5.5$, $\kappa = 0.159$ and 0.160 is roughly $M_K = 860$ MeV and 650 MeV respectively; and at $\beta = 5.6$, $\kappa = 0.156$ and 0.157 it is about 1050 MeV and 820 MeV respectively. This calculation of B_K has been done only with kaons created with a γ_5 operator. We find that a time interval of 16 is large enough

to give a stable plateau over about 6 central time-slices for both $\vec{p} = (0,0,0)$ and $(0,0,1)$ correlators, as illustrated in Figs. 5 and 6. The behavior of individual $B_{\mathcal{O}}$ terms is very similar to the quenched numbers shown in Tables 2a–3b.

Before presenting the final results, we first discuss a technical drawback of this calculation. On these lattices only Wuppertal source correlators are available, so with our method some contamination from higher momentum kaon states is present in the data. For momentum transfer $\vec{p} = (0,0,0)$, the largest contamination comes from the propagation of $\vec{p} = (0,0,1)$ kaons across the lattice. (The contamination in the $\vec{p} = (0,0,0) \to (0,0,1)$ data comes from the presence of $\vec{p} = (0,0,1) \to (0,0,2)$ terms.) This contribution is suppressed by two factors: the exponential suppression due to the extra energy of the $\vec{p} = (0,0,1)$ state, and the square of the ratio of amplitudes for creating a $\vec{p} = (0,0,1)$ kaon versus a $\vec{p} = (0,0,0)$ kaon by the Wuppertal source. These factors increase as the kaon mass decreases. They are similar on our four sets of lattices. At $\beta = 5.6$ and $\kappa = 0.157$, our estimates are ≈ 10 and $(1.5)^2$. There is also an enhancement factor because the matrix element between higher momentum kaon states is larger. We estimate this factor using VSA to be $(E(p=1)/M_K)^2 \approx (1.5)^2$. These three factors combine to increase the result for B_K by roughly 10%. We note that in the case of the quenched lattices, having 40 time-slices reduced this contamination to the level of a few percent. This is evident on comparing the $S-S$ and the $S-W$ or the $W-W$ results in Tables 2a-3b.

We again calculate B_K^L for three values of the effective coupling: 0.0, g^2 and $1.75g^2$. The lattice scale on individual lattices (without extrapolation to the chiral limit) is not well defined, and we simply set $\mu a = 1$. The results are shown in Table 6. As explained above, the results for B_K are likely to be $\sim 10\%$ larger due to contamination from higher momentum kaon states. In addition, B_K has to be extrapolated to the physical kaon mass. Thus, the only conclusion we can draw is that the quenched and dynamical results are in qualitative agreement for quarks masses in the range $m_s < m_q < 3m_s$.

7. B-parameter for the Left-Right electromagnetic penguins

There are two additional 4-fermion operators that we analyze using the data in Tables 2a-3b. These are the $\Delta I = 3/2$ part of the left-right electromagnetic penguin operators $\mathcal{O}_7$ and $\mathcal{O}_8$. They alone contribute to the imaginary part of the $I = 2$ amplitude and therefore give the dominant electromagnetic contribution to ϵ'/ϵ. A knowledge of their B-parameters is phenomenologically important as discussed in Ref. [23]. Taking just the $\Delta I = 3/2$ part

of the operators simplifies the numerical calculation as the "eye" contractions cancel in the flavor SU(2) limit.

In principle one would like to calculate the matrix elements of the penguin operators

$$\mathcal{O}_7 = (\bar{s}_a\gamma_\mu L d_a)\ \big[(\bar{u}_b\gamma_\mu R u_b) - \frac{1}{2}(\bar{d}_b\gamma_\mu R d_b) - \frac{1}{2}(\bar{s}_b\gamma_\mu R s_b)\big], \tag{7.1}$$

$$\mathcal{O}_8 = (\bar{s}_a\gamma_\mu L d_b)\ \big[(\bar{u}_b\gamma_\mu R u_a) - \frac{1}{2}(\bar{d}_b\gamma_\mu R d_a) - \frac{1}{2}(\bar{s}_b\gamma_\mu R s_a)\big], \tag{7.2}$$

between a K^+ and a π^+. Instead, we calculate the $\Delta I = 3/2$ part given by the operators

$$\mathcal{O}_7^{3/2} = (\bar{s}_a\gamma_\mu L d_a)\ \big[(\bar{u}_b\gamma_\mu R u_b) - (\bar{d}_b\gamma_\mu R d_b)\ \big] + (\bar{s}_a\gamma_\mu L u_a)(\bar{u}_b\gamma_\mu R d_b), \tag{7.3}$$

$$\mathcal{O}_8^{3/2} = (\bar{s}_a\gamma_\mu L d_b)\ \big[(\bar{u}_b\gamma_\mu R u_a) - (\bar{d}_b\gamma_\mu R d_a)\ \big] + (\bar{s}_a\gamma_\mu L u_b)(\bar{u}_b\gamma_\mu R d_a). \tag{7.4}$$

Note that the overall normalization is unimportant as it cancels in the B-parameters. The 1-loop perturbatively corrected versions of these operators have been calculated in Refs. [11] [12], and are linear combinations of the operators labeled $\mathcal{O}_1$ and $\mathcal{O}_2$ therein. The matrix elements of these corrected operators between a K^+ and a π^+ are, in the flavor SU(2) limit,

$$\begin{aligned}\mathcal{M}_7(\vec{p}) =& \left(1 + \frac{g^2}{16\pi^2} Z_1(r, a\mu)\right)\Big[2\mathcal{P}^1 - 2\mathcal{S}^1 + \mathcal{V}^2 - \mathcal{A}^2\Big] \\ &+ \frac{g^2}{16\pi^2}\,\frac{(Z_2 - Z_1)}{3}\Big[2\mathcal{P}^2 - 2\mathcal{S}^2 + \mathcal{V}^1 - \mathcal{A}^1\Big] \\ &+ \frac{g^2}{16\pi^2}\,\frac{r^2 Z^*(r)}{12}\Big[4\mathcal{P}^1 - 12\mathcal{P}^2 + 16\mathcal{S}^1 - 16\mathcal{S}^2 \\ &\qquad - 7\mathcal{V}^1 - 11\mathcal{V}^2 - 9\mathcal{A}^1 - 5\mathcal{A}^2 - 6\mathcal{T}^1 + 2\mathcal{T}^2\Big].\end{aligned} \tag{7.5}$$

and

$$\begin{aligned}\mathcal{M}_8(\vec{p}) =& \left(1 + \frac{g^2}{16\pi^2} Z_2(r, a\mu)\right)\Big[2\mathcal{P}^2 - 2\mathcal{S}^2 + \mathcal{V}^1 - \mathcal{A}^1\Big] \\ &+ \frac{g^2}{16\pi^2}\,\frac{r^2 Z^*(r)}{12}\Big[18\mathcal{P}^1 - 38\mathcal{P}^2 + 14\mathcal{S}^1 - 26\mathcal{S}^2 \\ &\qquad - 5\mathcal{V}^1 - \mathcal{V}^2 + \mathcal{A}^1 - 3\mathcal{A}^2 - 16\mathcal{T}^1\Big].\end{aligned} \tag{7.6}$$

where, if necessary, we have made a spin Fierz transformation to recast all the terms as two-spinor loops. The corresponding VSA contractions are

$$\mathcal{M}_7^{VSA}(\vec{p}) = \left[\frac{2}{3} Z_P^2\,\mathcal{P}^2 - Z_A^2\,\mathcal{A}^2\right], \tag{7.7}$$

and

$$\mathcal{M}_8^{VSA}(\vec{p}) = \left[2Z_P^2\,\mathcal{P}^2 - \frac{1}{3}Z_A^2\,\mathcal{A}^2\right]. \tag{7.8}$$

The B-parameters are the ratios of, for example, the matrix element of O_7 to its VSA. We evaluate these in the SU(3) limit, *i.e.* degenerate u, d and s quarks. The 1-loop values of the renormalization constants for these LR operators are also given in Table 1. Note that in the $DRED$ scheme the operator $\mathcal{O}_8^{3/2}$ does not mix with the scheme dependent operator $\bar{\mathcal{O}}$ of Ref. [12]. It is for this reason that we choose this scheme, although, our analysis shows that the results are only weakly scheme dependent.

In the chiral limit these matrix elements are expected to behave as $c + dm_\pi^2 + \ldots$. There are $O(a)$ corrections in the coefficients c and d due to the lattice discretization. At present the only way to reduce these is to use an improved action and/or work at weaker coupling. In this study we do not have any control over these corrections and we simply give the lattice results for the Wilson action.

The quality of the signal is shown in Figs. 7 and 8. In the analysis of these LR operators we find that using the full covariance matrix produced estimates that are about 1σ lower than the fit values shown unless we significantly decrease the range of the fit. The error estimates with and without using the full covariance matrix in the fits are essentially the same. This indicates that the data at different time slices is highly correlated and larger statistics is needed to reliably include the correlations. We choose to use the full range of the plateau in the fit and quote results obtained without including the correlations.

As in the case of the LL operator, in order to quote a value for the B-parameters we have to specify the value of $g^2_{\rm eff}$ and μa used in the perturbatively improved operators. In Table 7 we quote results for a number of choices in order to give an estimate of the sensitivity of the results to variation in these parameters. The data show that this could be a 10% effect, so it is important to make a good choice of $g^2_{\rm eff}$.

The data also show a small increase in the B-parameters as the quark mass is decreased. Linearly extrapolating the $g^2_{\rm eff} = 1.75$, $\mu a = \pi$ results to the physical kaon mass, our best estimates are

$$\begin{aligned} B_7^{3/2} &= 0.89(4), \\ B_8^{3/2} &= 0.93(5). \end{aligned} \tag{7.9}$$

These values are slightly smaller than the numbers used by Lusignoli *et al.* [23] in their analysis of ϵ'/ϵ; they used $B_7^{3/2} = B_8^{3/2} = 1.0 \pm 0.1$. To make a complete determination of ϵ'/ϵ we need to calculate many other matrix elements, for example of the strong penguin

operators $\mathcal{O}_5$ and $\mathcal{O}_6$, for which the lattice technology is still unreliable. For this reason we do not consider it opportune to repeat the phenomenological analysis.

We can make a direct comparison of lattice results for $\mathcal{O}_7^{3/2}$ with those obtained by Bernard and Soni on the subset of lattices described in the analysis of B_K. Their result, obtained using $g^2_{\rm eff} = 1.338$ and $\mu a = 1.7\pi$ in the $DR(\overline{EZ})$ scheme, is 0.965(41) at $\kappa = 0.155$, to be compared with 0.971(50) obtained by us. This comparison suggests that for the matrix elements of LR operators, our method of sandwiching the operator between smeared sources is no better than using propagators from a single source point. On the other hand the fact that smeared sources yield a plateau over a large range of time-slices gives reassurance that one potential source of systematic error is under control.

8. Conclusions

We show that the calculation of the kaon B-parameters with Wilson fermions is significantly improved by the use of non-local quark sources. By using a combination of Wuppertal and wall source correlators, we demonstrate that the on-shell matrix elements can be calculated at non-zero momenta.

By combining results at $\vec{p} = (0,0,0)$ and $(0,0,1)$, we carry out a non-perturbative subtraction of the lattice artifacts in the calculation of B_K. Even though we cannot take into account the artifact γ, our results are in good agreement with those obtained with staggered fermions. On the basis of this exploratory study we feel confident that the momentum subtraction procedure indeed works. To make further improvements and reduce the $O(a)$ artifacts one needs to repeat the calculations with an improved lattice action and on a larger physical lattice with smaller $\vec{p}_{min}$.

We find a clean plateau in the data for the B-parameters of the LR electromagnetic penguin operators. The results show that VSA works much better for these operators. All the B-parameters vary significantly with the choice of $g^2_{\rm eff}$ used in the perturbative renormalization coefficients. Our final estimates are given using the value advocated by Lepage and Mackenzie in Ref. [18], *i.e.* $g^2_{\rm eff} = 1.75$.

The method of using the combination of Wuppertal and wall correlators can be extended to study other 3-point correlation functions, in particular structure functions and form factors. This work is in progress.

Acknowledgments

We thank C. Bernard and G. Martinelli for providing unpublished data and for discussions. The $16^3 \times 40$ lattices were generated at NERSC at Livermore using a DOE allocation. The calculation of quark propagators and the analysis has been done at the Pittsburgh Supercomputing Center, San Diego Supercomputer Center, NERSC and Los Alamos National Laboratory. We are very grateful to Jeff Mandula, Norm Morse, Ralph Roskies, Charlie Slocomb and Andy White for their support of this project. This research was supported in part by the National Science Foundation under Grant No. PHY89-04035. RG, GWK, AP and SRS thank Institute for Theoretical Physics, Santa Barbara for hospitality during part of this work. AP also thanks Los Alamos National Laboratory for hospitality during the course of this work. GWK is supported in part by DOE Outstanding Junior Investigator and NSF Presidential Young Investigator programs. SRS is supported in part by DOE contract DE-AC05-84ER40150 and by an Alfred P. Sloan Fellowship.

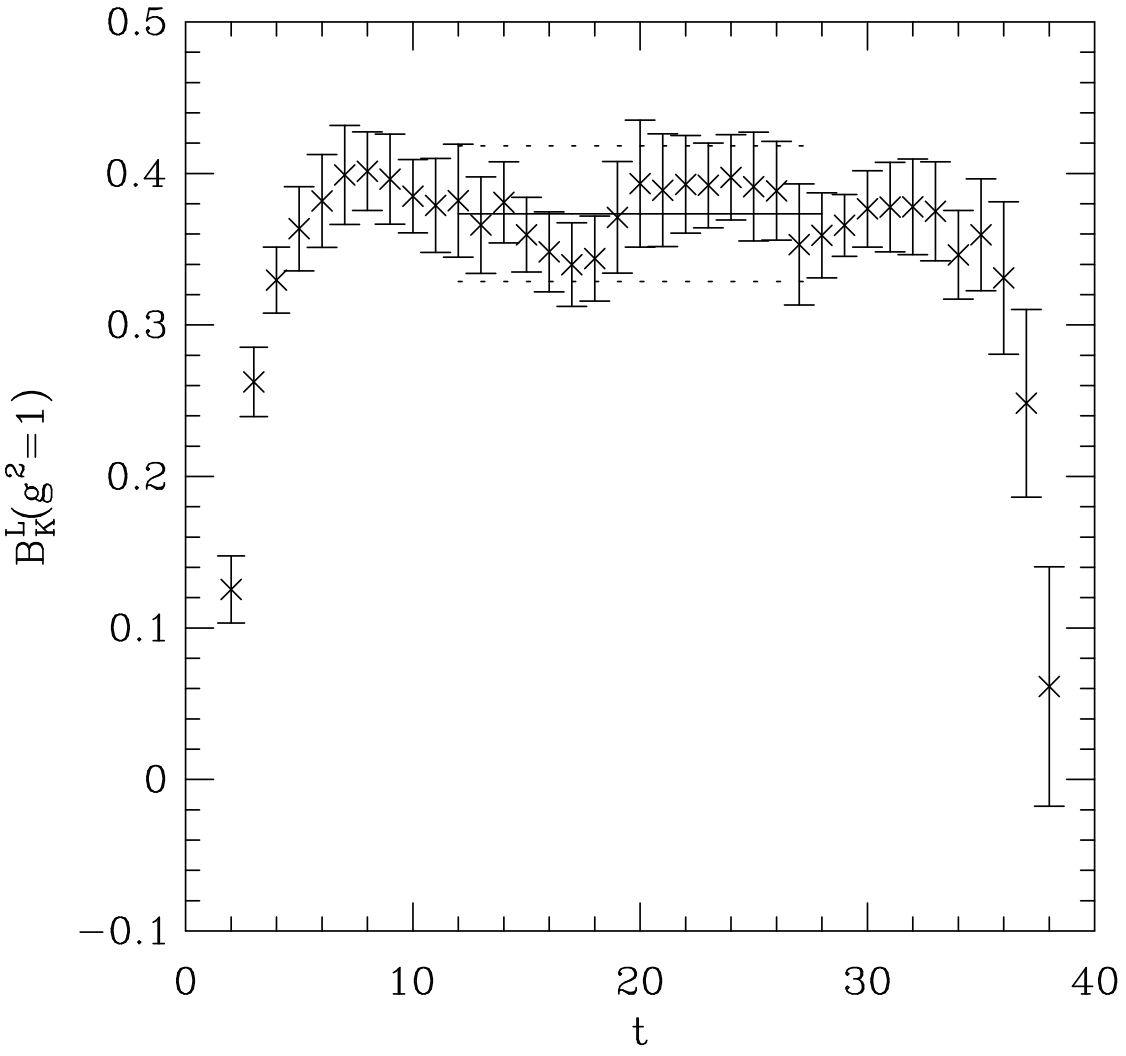

Fig. 1a. The ratio of correlators for the lattice parameter $B_K^L(g^2 = 1,\ \mu a = 1.0)$ at $\kappa = 0.154$ and for momentum transfer $\vec{p} = (0, 0, 0)$. The data are obtained using operator γ_5 as the kaon source.

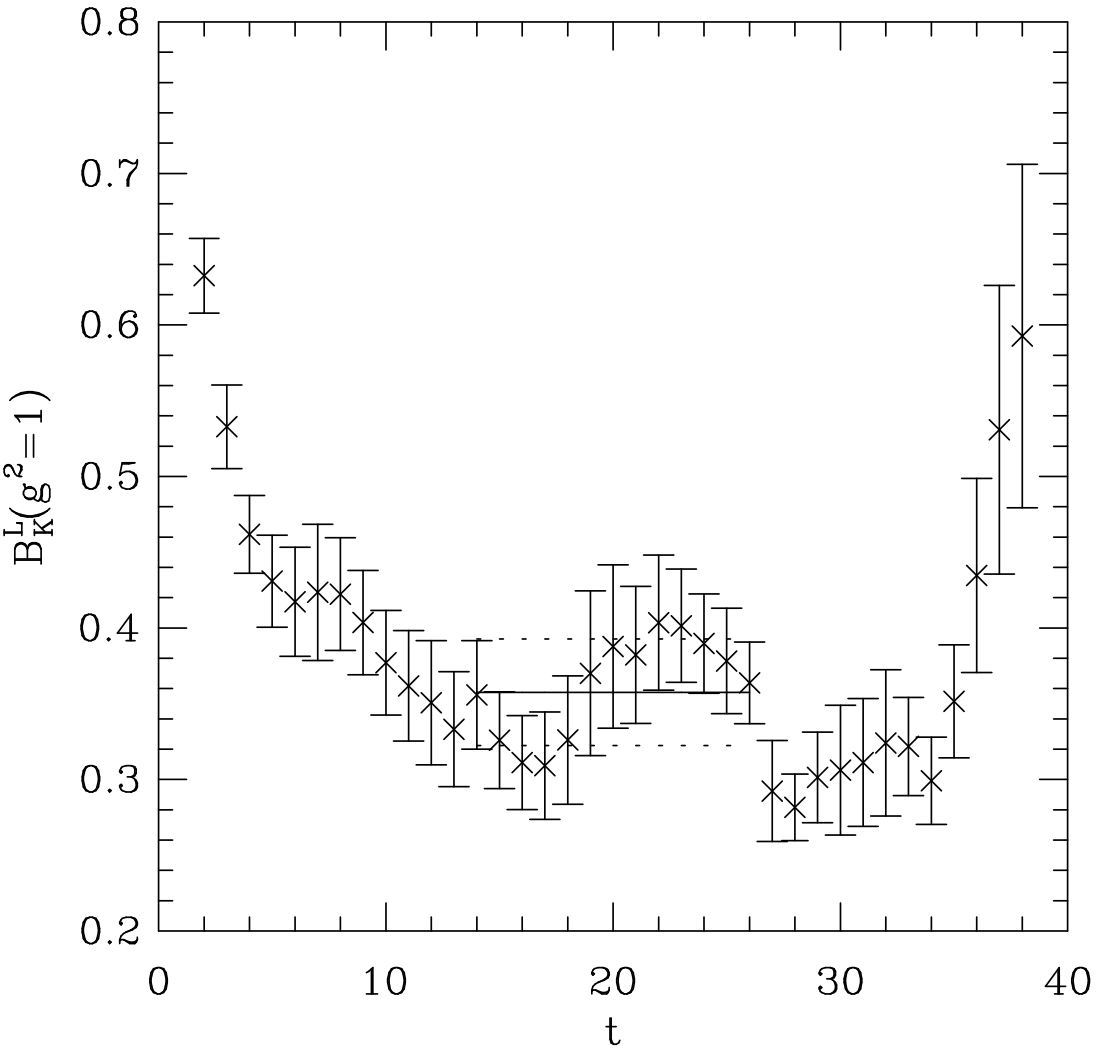

Fig. 1b. The same as in Fig. 1a, but using operator A_4 as the kaon source.

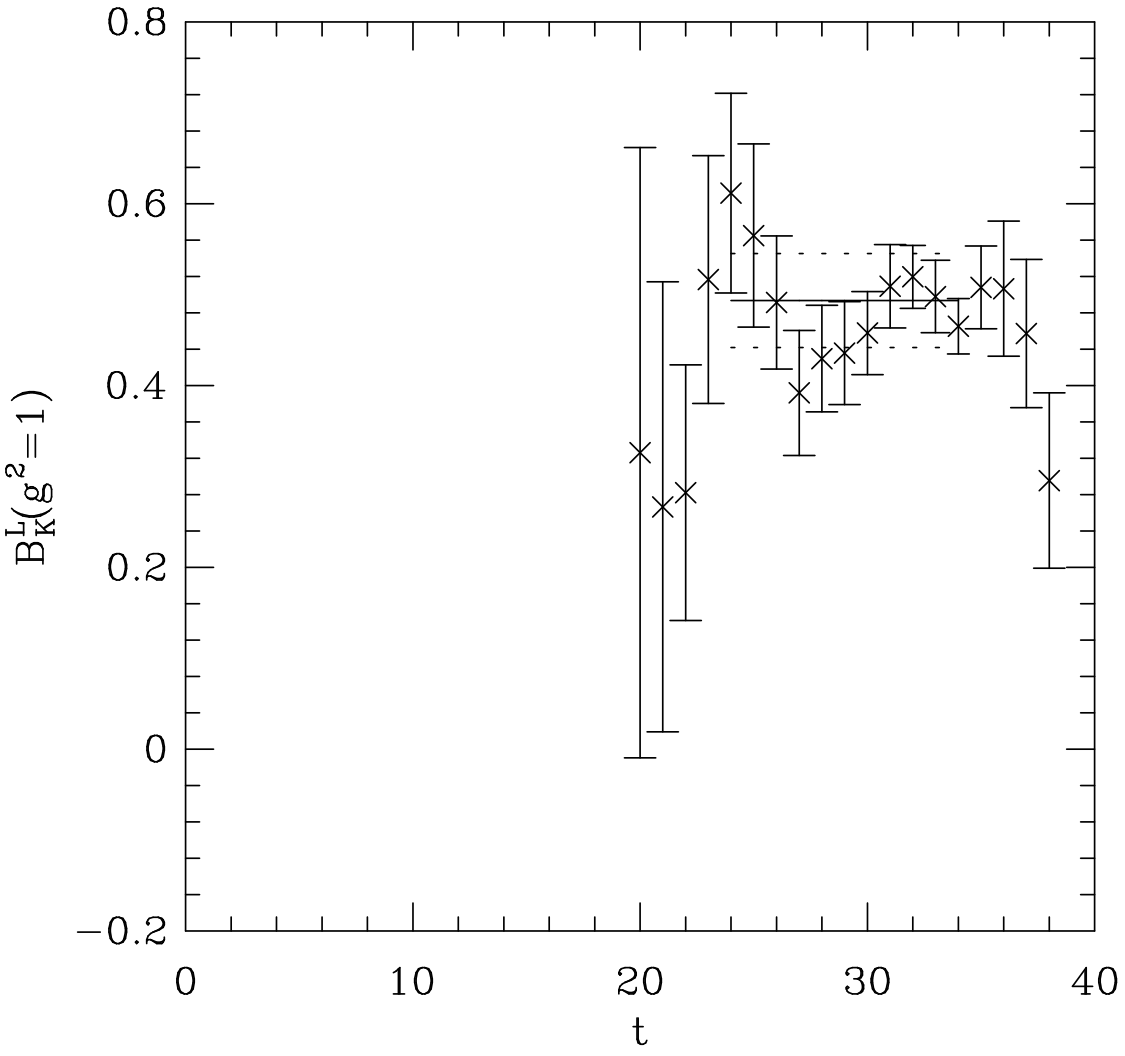

Fig. 2. The same as in Fig. 1a, but for $\kappa = 0.154$ and $\vec{p} = (0, 0, 1)$.

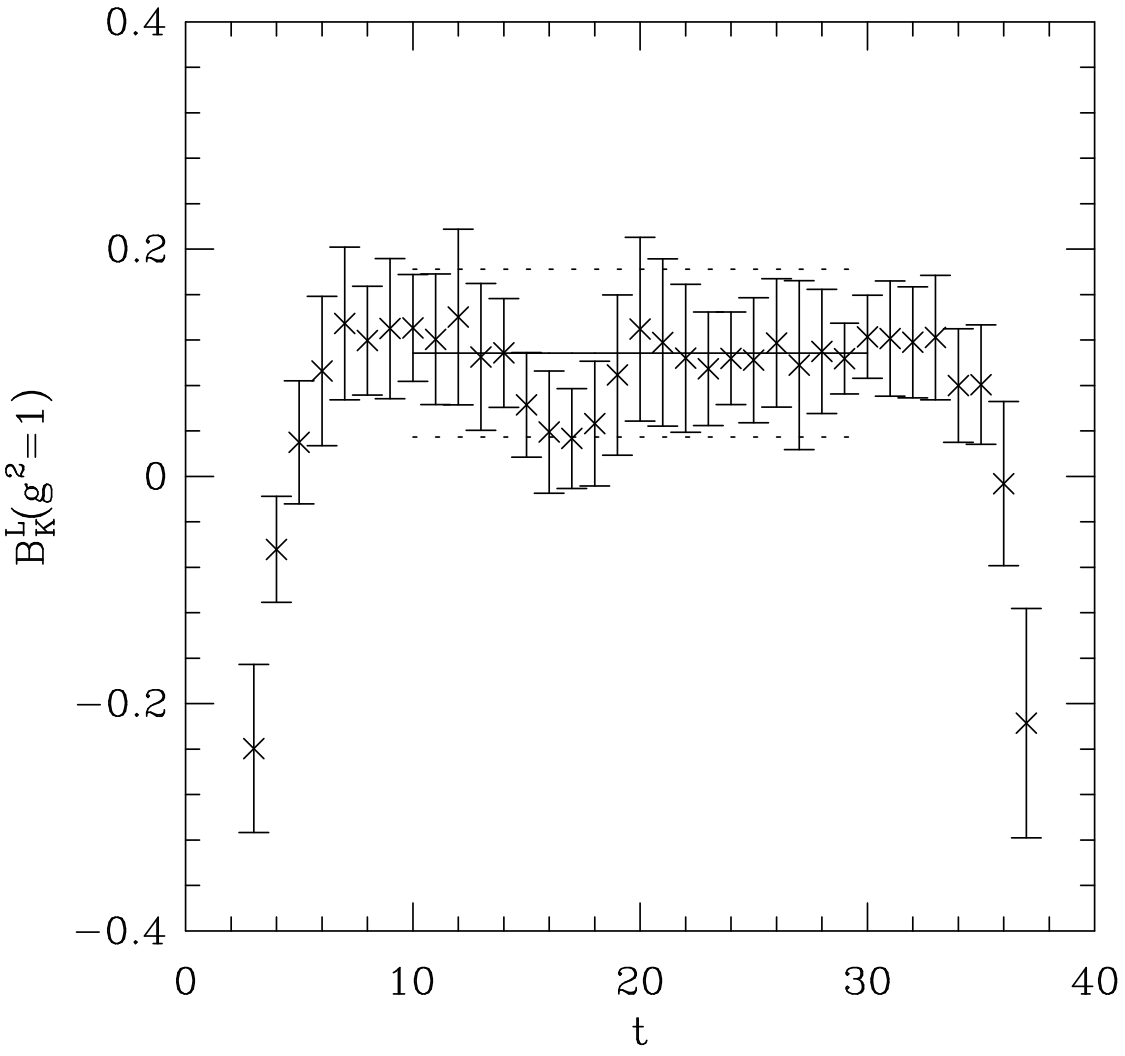

Fig. 3. The same as in Fig. 1a, but for $\kappa = 0.155$ and $\vec{p} = (0, 0, 0)$.

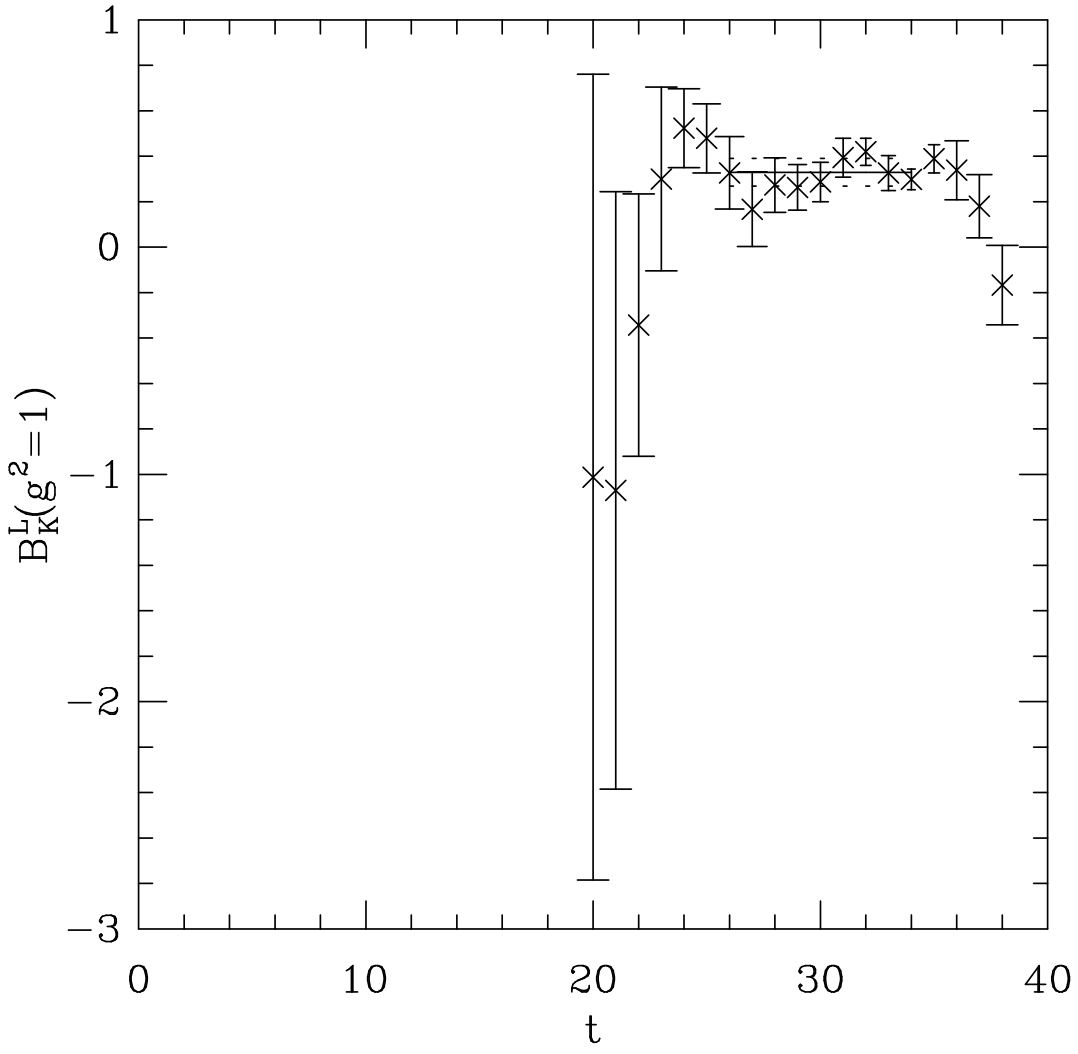

Fig. 4. The same as in Fig. 1a, but for $\kappa = 0.155$ and $\vec{p} = (0, 0, 1)$.

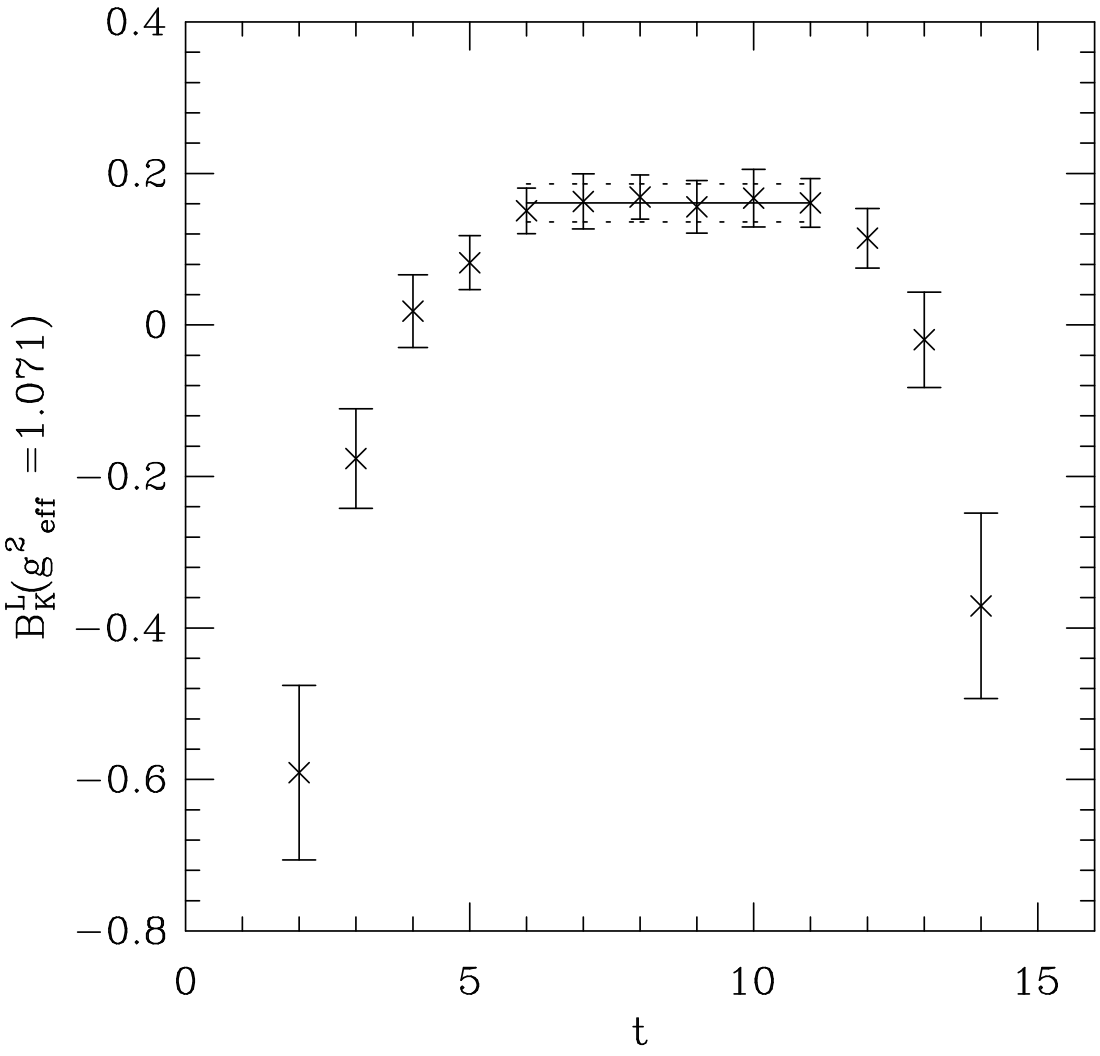

Fig. 5. The ratio of correlators for the lattice parameter $B_K^L(g^2_{\rm eff} = 1.071,\ \mu a = 1)$ measured on 16^4 lattices generated with two degenerate flavors of dynamical Wilson fermions. The lattice parameters are $\beta = 5.6$, $\kappa = 0.157$ and momentum transfer $\vec{p} = (0, 0, 0)$, and we use $\bar{s}\gamma_5 d$ as the kaon source.

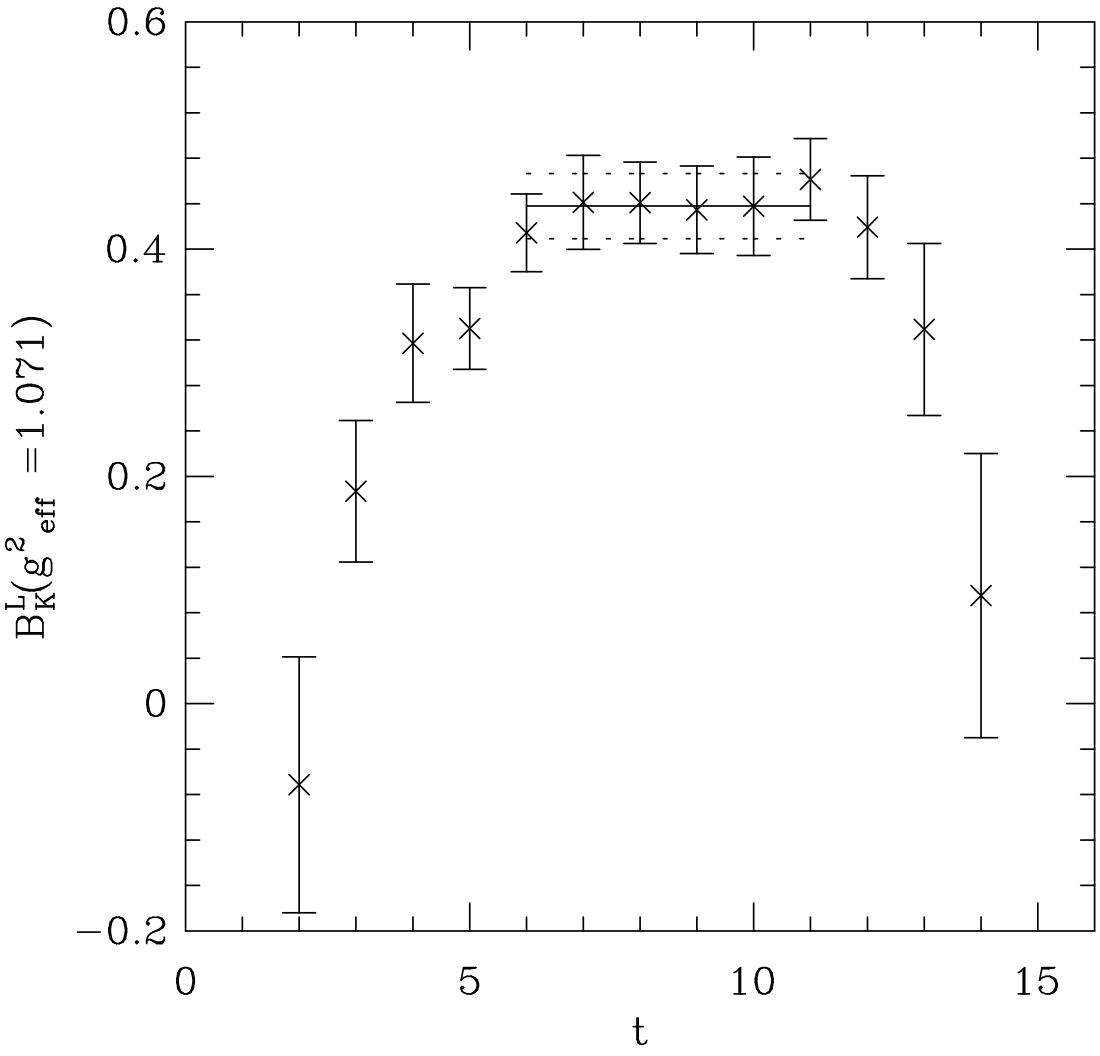

Fig. 6 The same as in Fig. 5, but for $\vec{p} = (0, 0, 1)$.

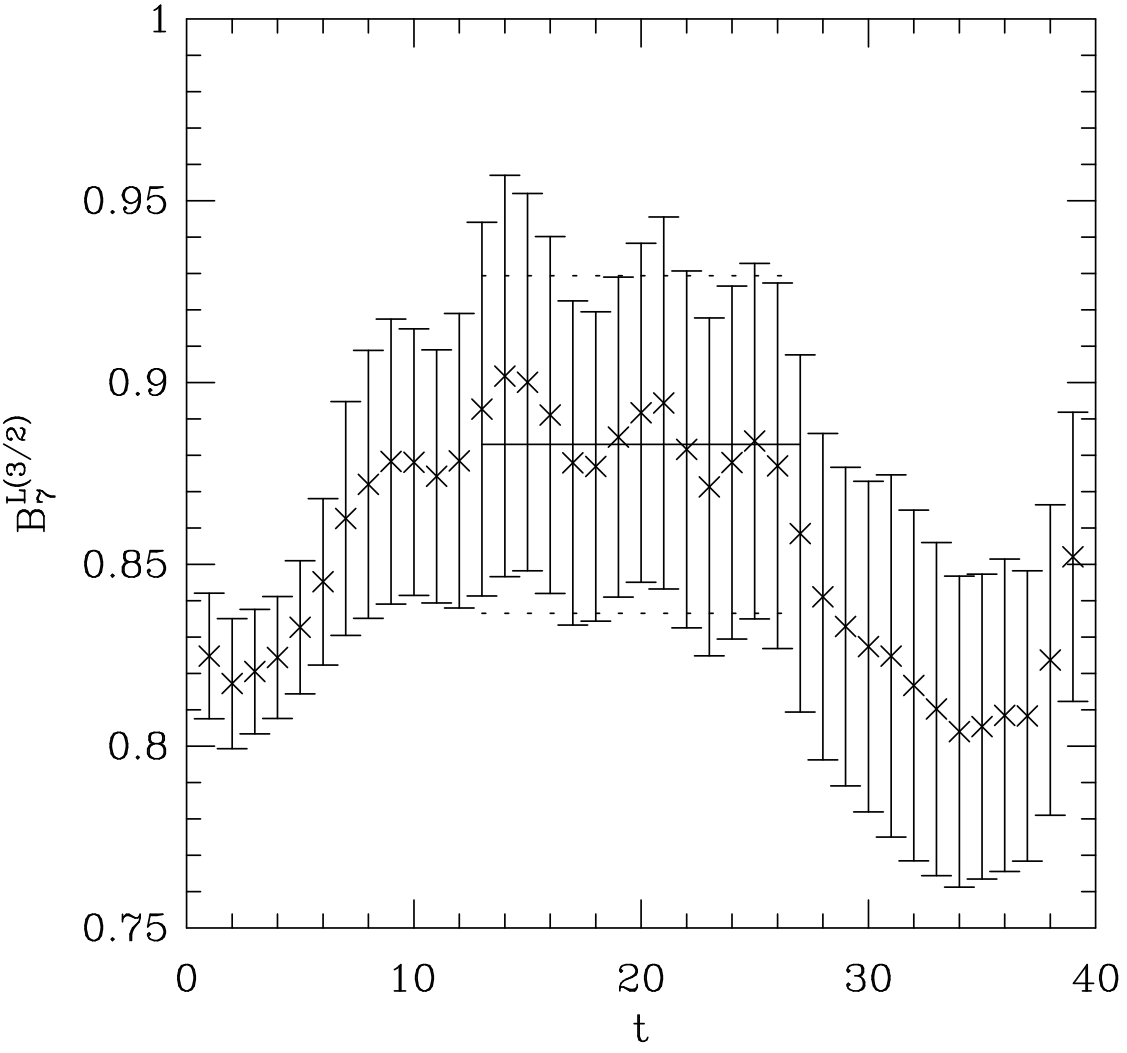

Fig. 7 B-parameter for the LR electromagnetic penguin operator $\mathcal{O}_7^{3/2}$. The data are obtained using $g^2_{\rm eff} = 1.75$ and $\mu a = \pi$.

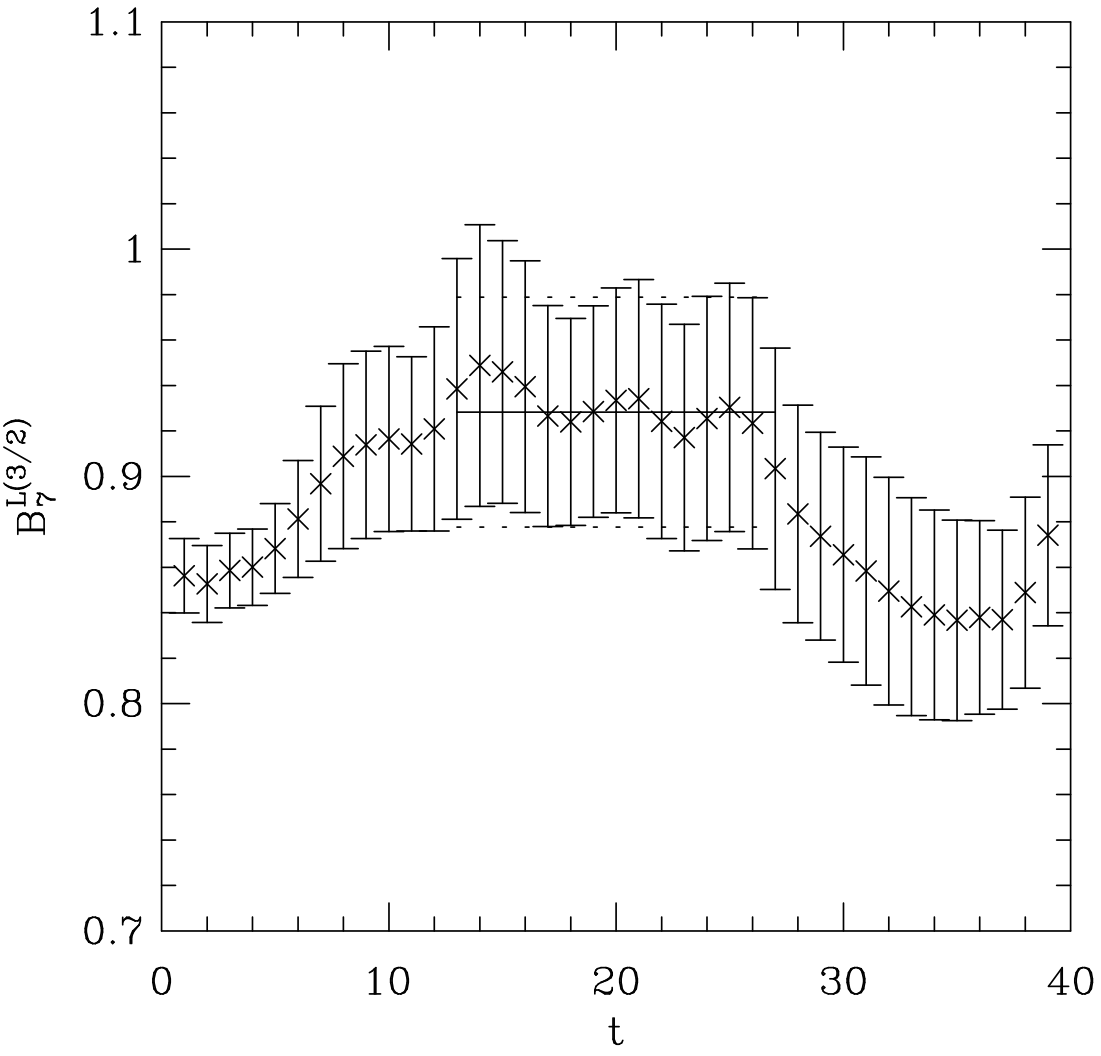

Fig. 8 B-parameter for the LR electromagnetic penguin operator $\mathcal{O}_8^{3/2}$. The data are obtained using $g^2_{\rm eff} = 1.75$ and $\mu a = \pi$.

	$DR(\overline{EZ})$	$DRED$	NDR
Z_A	$1 - 15.796 C_F\lambda$	$0.5 C_F\lambda$	0
Z_P	$1 + C_F\lambda(6\log(\mu a) - 21.596)$	0	$- C_F\lambda$
Z_+	$-50.174 - 4\log(\mu a)$	$\frac{7}{3}$	$\frac{14}{3}$
Z_-	$-45.308 + 8\log(\mu a)$	$-\frac{2}{3}$	$-\frac{4}{3}$
Z_1	$-49.364 - 2\log(\mu a)$	$\frac{11}{6}$	$\frac{11}{3}$
Z_2	$-42.064 + 16\log(\mu a)$	$-\frac{8}{3}$	$-\frac{16}{3}$
Z^*	9.6431	0	0

Table 1. Summary of 1-loop perturbative results for the various Z factors needed in our calculations in three different continuum regularization schemes. The two constants are $C_F = 4/3$ and $\lambda = g^2/(16\pi^2)$. The results in $DRED$ and NDR schemes are the sum of those in $DR(\overline{EZ})$ and the entries in their respective columns. These expressions are extracted from Refs. [11] [12] and [7]. The numerical results are taken from Ref. [12]. In the text all results are given in the $DRED$ scheme used in Ref. [11], except when we compare raw lattice numbers against those in Ref. [15].

	$PS[0]SP$	$PW[0]WP$	$PS[0]WP$	$PS[1]WP$	$AS[0]SA$	$AW[0]WA$	$AS[0]WA$	$AS[1]WA$
	1.6	1.1	0.3	0.8	1.4	1.2	0.6	0.5
	$14-26$	$14-26$	$14-26$	$23-31$	$12-28$	$14-26$	$10-30$	$22-31$
$\mathcal{P}^1$	$-4.30(21)$	$-4.03(17)$	$-3.99(19)$	$-2.58(28)$	$-3.86(35)$	$-3.86(21)$	$-3.70(20)$	$-2.45(27)$
	2.3	4.7	2.0	2.0	7.7	4.0	2.8	1.8
	$10-30$	$12-28$	$12-28$	$24-33$	$10-30$	$11-29$	$10-30$	$22-31$
$\mathcal{S}^1$	$-0.45(4)$	$-0.42(6)$	$-0.42(3)$	$-0.26(5)$	$-0.38(8)$	$-0.40(6)$	$-0.38(4)$	$-0.26(5)$
	2.2	6.0	4.3	1.2	4.0	6.1	3.2	1.8
	$16-28$	$12-28$	$13-27$	$26-33$	$10-30$	$10-30$	$10-30$	$22-32$
$\mathcal{V}_s^1$	0.40(18)	0.35(10)	0.35(8)	0.10(11)	0.36(9)	0.39(11)	0.31(6)	0.10(10)
	4.3	1.3	1.1	0.8	2.3	1.2	2.7	0.9
	$11-29$	$12-28$	$14-26$	$26-33$	$15-25$	$14-26$	$10-30$	$22-31$
$\mathcal{V}_t^1$	0.24(6)	0.22(2)	0.21(2)	0.12(2)	0.22(3)	0.20(2)	0.22(2)	0.11(3)
	3.5	2.0	2.2	0.2	2.2	2.7	2.0	0.4
	$12-28$	$12-28$	$11-29$	$25-34$	$10-30$	$14-26$	$10-30$	$26-33$
$\mathcal{A}_s^1$	$-0.60(6)$	$-0.56(6)$	$-0.56(5)$	$-0.33(4)$	$-0.54(3)$	$-0.50(5)$	$-0.52(6)$	$-0.28(6)$
	3.8	1.0	4.2	2.9	0.8	1.4	0.6	1.6
	$12-28$	$14-26$	$9-31$	$27-33$	$14-26$	$14-26$	$14-26$	$27-35$
$\mathcal{A}_t^1$	0.11(2)	0.12(2)	0.10(2)	0.15(3)	0.10(3)	0.12(2)	0.09(1)	0.15(4)
	1.8	1.5	0.9	1.9	0.6	2.8	1.1	0.7
	$10-30$	$15-25$	$10-30$	$25-34$	$16-24$	$12-28$	$10-30$	$23-31$
$\mathcal{T}_s^1$	2.84(21)	2.63(10)	2.70(10)	1.59(18)	2.56(34)	2.59(14)	2.51(16)	1.54(16)
	3.3	1.0	0.7	1.1	1.5	2.5	0.6	1.2
	$14-26$	$15-25$	$10-30$	$25-32$	$12-24$	$14-26$	$12-28$	$24-31$
$\mathcal{T}_t^1$	2.93(24)	2.73(10)	2.79(12)	1.70(21)	2.67(36)	2.66(17)	2.58(17)	1.66(20)

Table 2a. The one color loop contribution to the lattice $B-$parameters for individual operators at $\kappa = 0.154$. Each box shows the χ^2 for a correlated fit, the temporal range of the fit and the fitted value. The space and time components of the operators have been shown separately. The appropriate ratios of correlators have been calculated using two different kaon operators, γ_5 and A_4, and using Wuppertal and wall sources. The notation, for example, is: $PS[1]WP$ stands for the four-fermion operator with one unit of lattice momentum sandwiched between Wuppertal and wall source kaons each created with operator γ_5. All errors are calculated using the single elimination jackknife method.

	$PS[0]SP$	$PW[0]WP$	$PS[0]WP$	$PS[1]WP$	$AS[0]SA$	$AW[0]WA$	$AS[0]WA$	$AS[1]WA$
	1.6	0.9	0.4	0.8	1.6	1.1	0.8	0.6
	$12-28$	$12-28$	$10-30$	$23-32$	$12-28$	$14-26$	$9-31$	$22-31$
$\mathcal{P}^2$	$-12.09(75)$	$-11.60(50)$	$-11.26(43)$	$-7.15(75)$	$-10.99(95)$	$-11.05(60)$	$-10.77(54)$	$-6.81(68)$
	2.9	2.7	2.8	1.7	2.7	1.3	2.0	1.8
	$10-30$	$14-26$	$14-26$	$25-33$	$12-28$	$14-26$	$10-30$	$22-31$
$\mathcal{S}^2$	$-0.60(10)$	$-0.51(9)$	$-0.49(6)$	$-0.40(8)$	$-0.47(14)$	$-0.49(6)$	$-0.52(7)$	$-0.38(7)$
	1.2	1.3	1.1	0.6	3.0	2.5	1.6	1.6
	$15-25$	$14-26$	$12-28$	$25-34$	$10-30$	$14-32$	$10-32$	$26-33$
$\mathcal{V}_s^2$	0.03(3)	0.04(2)	0.05(2)	0.01(2)	0.04(3)	0.04(3)	0.04(2)	$-0.02(3)$
	1.0	2.1	1.8	1.3	2.8	2.1	2.2	1.5
	$14-26$	$14-26$	$10-30$	$25-34$	$12-28$	$14-26$	$10-30$	$24-31$
$\mathcal{V}_t^2$	0.02(0)	0.02(1)	0.02(0)	0.01(1)	0.02(0)	0.02(1)	0.02(0)	0.02(1)
	5.1	2.4	1.9	2.1	2.4	2.1	1.9	1.2
	$8-32$	$11-26$	$10-30$	$25-34$	$10-30$	$14-26$	$10-30$	$25-33$
$\mathcal{A}_s^2$	$-0.54(5)$	$-0.52(4)$	$-0.53(4)$	$-0.31(3)$	$-0.50(7)$	$-0.49(4)$	$-0.49(5)$	$-0.25(4)$
	3.4	4.2	1.3	0.8	2.8	3.3	0.7	0.8
	$13-24$	$10-25$	$15-25$	$25-33$	$12-24$	$14-26$	$16-24$	$24-32$
$\mathcal{A}_t^2$	0.64(4)	0.62(3)	0.58(2)	0.64(8)	0.56(5)	0.58(7)	0.54(3)	0.60(7)
	5.3	3.6	3.2	2.0	3.6	3.9	3.0	1.5
	$10-30$	$12-28$	$10-30$	$28-34$	$12-28$	$14-26$	$10-30$	$23-35$
$\mathcal{T}_s^2$	0.05(2)	0.06(2)	0.05(1)	0.03(1)	0.05(2)	0.05(1)	0.04(2)	0.04(1)
	7.1	1.5	2.3	1.0	3.7	2.1	4.1	1.1
	$14-26$	$14-26$	$10-30$	$25-33$	$8-31$	$14-26$	$6-34$	$26-33$
$\mathcal{T}_t^2$	0.07(2)	0.05(1)	0.05(1)	0.03(1)	0.03(5)	0.04(3)	0.06(2)	0.05(1)

Table 2b. The same as Table 2a, but for the two color loop contribution.

	$PS[0]SP$	$PW[0]WP$	$PS[0]WP$	$PS[1]WP$	$AS[0]SA$	$AW[0]WA$	$AS[0]WA$	$AS[1]WA$
	2.6	0.6	0.5	2.1	1.9	1.8	0.9	0.8
	$10-30$	$16-27$	$10-30$	$23-33$	$12-28$	$14-28$	$12-30$	$26-33$
$\mathcal{P}^1$	$-7.08(97)$	$-6.48(41)$	$-6.49(39)$	$-3.42(57)$	$-5.98(71)$	$-5.99(44)$	$-5.58(42)$	$-3.24(42)$
	3.2	4.4	1.8	1.4	4.5	3.4	1.5	2.3
	$10-30$	$14-27$	$11-29$	$28-33$	$10-30$	$14-28$	$12-30$	$26-33$
$\mathcal{S}^1$	$-1.01(18)$	$-0.92(19)$	$-0.94(10)$	$-0.48(13)$	$-0.85(14)$	$-0.89(19)$	$-0.85(10)$	$-0.48(11)$
	5.9	8.7	3.1	1.2	4.6	10.6	3.3	1.1
	$13-29$	$13-27$	$13-27$	$25-33$	$14-32$	$10-30$	$12-30$	$27-34$
$\mathcal{V}_s^1$	0.83(65)	0.87(41)	0.91(17)	0.32(18)	0.83(18)	0.83(31)	0.79(18)	0.36(27)
	6.0	2.9	1.5	1.1	5.3	1.5	1.0	0.5
	$15-26$	$11-29$	$14-26$	$26-33$	$11-30$	$14-28$	$13-29$	$26-33$
$\mathcal{V}_t^1$	0.38(15)	0.45(9)	0.42(5)	0.22(6)	0.42(9)	0.41(8)	0.40(5)	0.23(7)
	4.4	2.6	1.6	0.3	0.7	3.9	2.2	0.8
	$10-30$	$12-28$	$14-27$	$27-33$	$8-32$	$12-28$	$10-30$	$26-33$
$\mathcal{A}_s^1$	$-1.02(17)$	$-1.09(20)$	$-1.01(12)$	$-0.49(15)$	$-0.92(12)$	$-0.97(19)$	$-0.89(10)$	$-0.38(14)$
	0.3	4.3	2.9	3.0	1.7	4.2	1.8	2.1
	$12-28$	$10-30$	$12-28$	$28-33$	$10-28$	$13-27$	$14-27$	$25-34$
$\mathcal{A}_t^1$	0.01(5)	$-0.01(3)$	$-0.03(3)$	0.12(7)	$-0.01(4)$	0.02(5)	$-0.01(3)$	0.14(9)
	3.9	4.9	0.9	1.8	1.2	4.0	1.1	0.9
	$12-28$	$12-30$	$11-29$	$26-33$	$12-24$	$14-28$	$11-29$	$26-33$
$\mathcal{T}_s^1$	5.66(69)	5.09(59)	5.27(30)	2.73(52)	4.90(91)	4.79(66)	4.75(39)	2.76(47)
	4.0	2.9	0.7	2.3	2.5	3.1	1.3	1.5
	$12-28$	$13-30$	$12-28$	$26-33$	$13-25$	$14-28$	$10-30$	$26-33$
$\mathcal{T}_t^1$	5.86(77)	5.39(49)	5.38(32)	3.24(48)	4.87(121)	5.01(46)	4.93(30)	2.96(48)

Table 3a. The same as in Table 2a, but for $\kappa = 0.155$.

	$PS[0]SP$	$PW[0]WP$	$PS[0]WP$	$PS[1]WP$	$AS[0]SA$	$AW[0]WA$	$AS[0]WA$	$AS[1]WA$
	2.6	2.7	0.6	1.0	2.0	1.6	0.9	0.8
	$10-30$	$13-29$	$10-30$	$24-32$	$12-28$	$14-28$	$11-29$	$26-33$
$\mathcal{P}^2$	$-19.7(26)$	$-18.4(15)$	$-18.0(11)$	$-9.0(15)$	$-16.7(23)$	$-16.8(13)$	$-15.8(12)$	$-9.0(11)$
	2.7	4.0	2.4	1.3	2.2	3.3	1.1	2.2
	$10-30$	$13-27$	$10-30$	$26-35$	$12-28$	$14-28$	$15-27$	$26-33$
$\mathcal{S}^2$	$-1.45(32)$	$-1.44(33)$	$-1.43(17)$	$-0.94(23)$	$-0.98(31)$	$-1.24(14)$	$-1.05(24)$	$-0.82(15)$
	5.2	3.9	1.0	1.4	1.6	2.5	1.0	1.6
	$11-29$	$14-28$	$12-26$	$26-33$	$14-27$	$16-30$	$12-28$	$27-32$
$\mathcal{V}_s^2$	0.07(4)	0.06(4)	0.08(2)	0.00(4)	0.13(11)	0.02(7)	0.05(4)	$-0.08(9)$
	3.8	3.4	2.0	1.4	4.6	4.3	1.7	1.3
	$12-28$	$14-27$	$10-30$	$26-33$	$14-27$	$14-28$	$15-27$	$26-31$
$\mathcal{V}_t^2$	0.04(1)	0.04(1)	0.04(1)	0.01(1)	0.02(3)	0.04(2)	0.03(1)	0.03(2)
	7.4	3.6	2.5	1.8	2.8	1.5	1.4	1.3
	$12-28$	$11-31$	$10-30$	$26-35$	$14-27$	$15-27$	$11-29$	$26-34$
$\mathcal{A}_s^2$	$-1.06(17)$	$-0.96(6)$	$-0.97(9)$	$-0.52(9)$	$-0.89(14)$	$-0.86(8)$	$-0.87(13)$	$-0.42(8)$
	0.1	3.9	1.9	1.2	0.3	5.9	1.4	1.1
	$12-28$	$15-25$	$16-24$	$26-33$	$12-28$	$14-28$	$12-25$	$28-34$
$\mathcal{A}_t^2$	0.57(10)	0.51(9)	0.49(9)	0.61(13)	0.49(10)	0.48(11)	0.45(4)	0.53(8)
	4.0	3.3	2.6	2.2	4.2	3.8	4.1	2.1
	$15-25$	$13-27$	$14-27$	$28-34$	$12-28$	$14-28$	$9-31$	$26-33$
$\mathcal{T}_s^2$	0.14(6)	0.13(3)	0.14(3)	0.03(2)	0.09(3)	0.11(3)	0.11(4)	0.06(3)
	4.4	1.6	2.6	1.0	1.9	3.0	1.8	0.8
	$14-27$	$14-27$	$12-28$	$26-33$	$14-26$	$17-26$	$10-30$	$26-35$
$\mathcal{T}_t^2$	0.15(4)	0.14(1)	0.14(2)	0.05(2)	0.06(5)	0.12(8)	0.13(4)	0.07(2)

Table 3b. The same as Table 3a, but for the two color loop contribution.

		$\kappa = 0.154$			$\kappa = 0.155$		
g^2_{eff}	μa	$B_K^L(\vec{p}=0)$ $12-28$	$B_K^L(\vec{p}=1)$ $24-34$	B_K	$B_K^L(\vec{p}=0)$ $10-30$	$B_K^L(\vec{p}=1)$ $26-34$	B_K
0.00	–	0.298(44)	0.446(42)	0.83(21)	− 0.023(63)	0.263(62)	0.77(19)
1.00	1.0	0.373(45)	0.494(52)	0.81(23)	0.109(74)	0.330(61)	0.71(20)
1.00	π	0.362(42)	0.476(50)	0.78(22)	0.110(71)	0.319(60)	0.69(22)
1.00	1.7π	0.356(42)	0.468(50)	0.76(22)	0.110(70)	0.315(59)	0.67(21)
1.338	1.0	0.405(44)	0.512(55)	0.79(24)	0.175(75)	0.359(69)	0.68(24)
1.338	π	0.388(42)	0.486(53)	0.75(22)	0.176(71)	0.344(62)	0.64(22)
1.338	1.7π	0.380(41)	0.475(51)	0.72(22)	0.176(69)	0.337(61)	0.62(22)
1.75	1.0	0.453(45)	0.536(58)	0.75(23)	0.268(70)	0.401(74)	0.64(25)
1.75	π	0.429(42)	0.497(53)	0.68(22)	0.268(63)	0.379(71)	0.57(23)
1.75	1.7π	0.417(41)	0.497(51)	0.64(21)	0.268(59)	0.369(69)	0.55(22)

Table 4. The lattice $B-$parameter for the perturbatively improved operator $\hat{\mathcal{O}}$ for zero and one unit of lattice momentum, and the B-parameter after momentum subtraction. The data show the magnitude of the variation with the value of $g^2_{\rm eff}$ and μa used in the perturbative renormalization constants. The range of time-slices used in the fits is specified in the header.

	Wilson $\kappa = 0.154$	Staggered $m_q = 0.02 + 0.03$	Wilson $\kappa = 0.155$	Staggered $m_q = 0.01 + 0.02$
M_K	0.370(6)	0.374(3)	0.297(11)	0.296(2)
E_K	0.511(12)		0.466(22)	
$\mathcal{V}_s^1$	−0.57(33)	−0.48(2)	−0.71(53)	−0.79(4)
$\mathcal{V}_s^2$	−0.11(8)	−0.036(4)	−0.13(11)	−0.10(1)
$\mathcal{V}_t^1$	−0.10(7)	−0.056(3)	−0.12(15)	−0.13(1)
$\mathcal{V}_t^2$	0.01(2)	−0.009(1)	−0.02(4)	−0.024(2)
$\mathcal{A}_s^1$	0.28(18)	0.15(1)	0.41(42)	0.36(2)
$\mathcal{A}_s^2$	0.27(16)	0.063(5)	0.29(32)	0.13(1)
$\mathcal{A}_t^1$	0.28(12)	0.33(1)	0.40(20)	0.42(1)
$\mathcal{A}_t^2$	0.79(26)	0.81(1)	0.82(40)	0.85(2)
$B_{\mathcal{A}}$	1.62(42)	1.35(3)	1.92(89)	1.76(5)
$B_{\mathcal{V}}$	−0.78(40)	−0.58(2)	−0.98(71)	−1.04(5)
B_K	0.83(21)	0.76(1)	0.77(19)	0.72(2)

Table 5. Comparison of individual $B-$parameters, for space/time and 1-loop/2-loop components of the vector and axial four-fermion operators, between Wilson and staggered fermions at matching values of the kaon mass. The kaon energy at $\vec{p} = (0,0,0)$ and $\vec{p} = (0,0,1)$ measured from the 2-point correlators is also given. All results are quoted for $g^2_{\rm eff} = 0$.

		$B_K^L(0)$	$B_K^L(1)$	M_K	$E(1)$	B_K
	$g^2_{eff} = 0.000$	0.327(88)	0.507(96)			0.98(43)
$\kappa = 0.159$	$g^2_{eff} = 1.091$	0.389(74)	0.537(80)	0.477(13)	0.660(16)	0.92(36)
	$g^2_{eff} = 1.909$	0.401(56)	0.505(58)			0.78(27)
	$g^2_{eff} = 0.000$	−0.593(88)	−0.052(51)			0.93(24)
$\kappa = 0.160$	$g^2_{eff} = 1.091$	−0.415(76)	0.051(44)	0.362(7)	0.562(22)	0.89(21)
	$g^2_{eff} = 1.909$	−0.217(57)	0.132(34)			0.76(17)
	$g^2_{eff} = 0.000$	0.497(33)	0.685(39)			1.23(20)
$\kappa = 0.156$	$g^2_{eff} = 1.071$	0.534(31)	0.693(36)	0.456(5)	0.613(10)	1.15(19)
	$g^2_{eff} = 1.875$	0.512(26)	0.629(30)			0.97(16)
	$g^2_{eff} = 0.000$	0.154(25)	0.436(29)			1.14(19)
$\kappa = 0.157$	$g^2_{eff} = 1.071$	0.161(25)	0.438(29)	0.358(7)	0.501(16)	1.13(19)
	$g^2_{eff} = 1.875$	0.234(21)	0.439(24)			0.95(16)

Table 6. The same as in Table 4, but for lattices generated with two flavors of dynamical Wilson quarks. The upper and lower halves of the table correspond to $\beta = 5.5$ and $\beta = 5.6$ respectively. These numbers are obtained with $\mu a = 1.0$.

		$\kappa = 0.154$		$\kappa = 0.155$	
g^2_{eff}	μa	$\mathcal{O}_7^{3/2}$	$\mathcal{O}_8^{3/2}$	$\mathcal{O}_7^{3/2}$	$\mathcal{O}_8^{3/2}$
0.00	–	0.902(24)	0.947(30)	0.908(44)	0.963(50)
1.00	1.0	0.871(24)	0.918(29)	0.878(44)	0.935(50)
1.00	π	0.918(29)	0.945(30)	0.911(46)	0.962(52)
1.00	1.7π	0.901(25)	0.953(30)	0.921(46)	0.969(52)
1.338	1.0	0.832(23)	0.877(23)	0.830(43)	0.894(48)
1.338	π	0.891(25)	0.934(30)	0.902(46)	0.951(51)
1.338	1.7π	0.908(25)	0.950(30)	0.921(47)	0.966(52)
1.75	1.0	0.747(21)	0.785(26)	0.753(40)	0.802(45)
1.75	π	0.869(25)	0.911(30)	0.883(46)	0.928(51)
1.75	1.7π	0.901(26)	0.941(31)	0.916(48)	0.958(52)

Table 7. The B-parameter for the LR electromagnetic penguin operators on the quenched lattices. The fit range is $t = 13 - 27$ in all cases. The results are shown for a number of values of g^2_{eff} and μa used in the perturbative renormalization constants.

References

[1] M.B. Gavela, *et al.*, *Nucl. Phys.* **B306** (1988) 677.

[2] C. Bernard and A. Soni, Int. Symp. *"LATTICE 89"*, Proceedings of the International Symposium on Lattice Field Theory, Capri, Italy, 1989, edited by N. Cabibbo *et al.*, *Nucl. Phys.* **B** *(Proc. Suppl.)* **17**, (1990) 495.

[3] G. Kilcup, S. Sharpe, R. Gupta and A. Patel, *Phys. Rev. Lett.* **64** (1990) 25.

[4] G. Martinelli, Int. Symp. *"LATTICE 89"*, Proceedings of the International Symposium on Lattice Field Theory, Capri, Italy, 1989, edited by N. Cabibbo *et al.*, *Nucl. Phys.* **B** *(Proc. Suppl.)* **17**, (1990) 523.

[5] G. Martinelli *et al.*, Roma preprint no. 850 (1991).

[6] S. Güsken *et al.*, *Phys. Lett.* **227B** (1989) 266;
S. Güsken, Int. Symp. *"LATTICE 89"*, Proceedings of the International Symposium on Lattice Field Theory, Capri, Italy, 1989, edited by N. Cabibbo *et al.*, *Nucl. Phys.* **B** *(Proc. Suppl.)* **17**, (1990) 365.

[7] D. Daniel, R. Gupta, G. Kilcup, A. Patel and S. Sharpe, *Phys. Rev.* **D46** (1992) 3130

[8] C. Bernard, T. Draper, G. Hockney and A. Soni, Int. Symp. *"Field theory on the Lattice"*, Proceedings of the International Symposium on Lattice Field Theory, Seillac, France, 1987, edited by A. Billoire *et al.*, *Nucl. Phys.* **B** *(Proc. Suppl.)* **4**, (1988) 483.

[9] E. Franco, L. Maiani, G. Martinelli and E. Morelli, *Nucl. Phys.* **B317** (1989) 63.

[10] S. Sharpe, R. Gupta, G. Guralnik, G. Kilcup and A. Patel, *Phys. Lett.* **192B** (1987) 149.

[11] G. Martinelli, *Phys. Lett.* **141B** (1984) 395.

[12] C. Bernard, T. Draper and A. Soni, *Phys. Rev.* **D36** (1987) 3224.

[13] G. Altarelli, G. Curci, G. Martinelli and S. Petrarca, *Nucl. Phys.* **B187** (1981) 461

[14] A. Buras and P. Weisz, *Nucl. Phys.* **B333** (1990) 66

[15] C. Bernard and A. Soni, private communications.

[16] C. Bernard and A. Soni, Int. Symp. *"LATTICE 88"*, Proceedings of the International Symposium on Lattice Field Theory, Fermilab, USA, 1988, edited by A.S. Kronfeld and P.B. Mackenzie, *Nucl. Phys.* **B** *(Proc. Suppl.)* **9** (1989) 155.

[17] S. Sharpe, Int. Symp. *"LATTICE 89"*, Proceedings of the International Symposium on Lattice Field Theory, Capri, Italy, 1989, edited by N. Cabibbo *et al.*, *Nucl. Phys.* **B** *(Proc. Suppl.)* **17**, (1990) 146.

[18] G.P. Lepage and P.B. Mackenzie, Int. Symp. *"LATTICE 90"*, Proceedings of the International Symposium on Lattice Field Theory, Tallahassee, Florida, USA, 1990, edited by U. M. Heller *et al.*, *Nucl. Phys.* **B** *(Proc. Suppl.)* **20**, (1991) 173; Fermilab preprint FERMILAB-PUB-19/355-T (9/92)

[19] R. Gupta, G. Guralnik, G.W. Kilcup, S. R. Sharpe, *Phys. Rev.* **D43** (1991) 2003.

[20] S. Sharpe, in *Standard Model, Hadron Phenomenology and Weak Decays on the Lattice*, Ed. G. Martinelli, World Scientific.

[21] S. Sharpe, *Phys. Rev.* **D46** (1992) 3146

[22] R. Gupta, C. Baillie, R. Brickner, G. Kilcup, A. Patel and S. R. Sharpe, *Phys. Rev.* **D44** (1991) 3272.

[23] M. Lusignoli, L. Maiani, G. Martinelli and L. Reina, *Nucl. Phys.* **B369** (1992) 139.